Review | Open Access

Chemical Synthesis

Tahir *et al. Chem. Synth.* **2026**, *6*, 62 **DOI:**10.20517/cs.2026.06

Single and dual atom catalysts for nitrate reduction from metal tuning to performance descriptors

Nadia Tahir[1], Pengcheng Guo[2,*], Tazeen Fatima[1], Muhammad Altaf Nazir[3], Khansa Pervaiz[1], Shabana Shaheen[4], Ghulam Murtaza[1], Tayyaba Najam[3,*], Xingke Cai[5,*], Syed Shoaib Ahmad Shah[1,6,*]

Keywords:
Single atom catalysts, dual atom catalysts, nitrate electroreduction, ammonia production

Citation: Tahir, N.; Guo, P.; Fatima, T.; Nazir, M. A.; Pervaiz, K.; Shaheen, S.; Murtaza, G.; Najam, T.; Cai, X.; Shah, S. S. A. Single and dual atom catalysts for nitrate reduction from metal tuning to performance descriptors. *Chem. Synth.* **2026**, *6*, 62. https://dx.doi.org/10.20517/cs.2026.06

Received: 15 Jan 2026
First Decision: 10 Feb 2026
Revised: 25 Jun 2026
Accepted: 29 Jun 2026
Published: 27 Jul 2026

Academic Editor:
Xiaoxin Zou
Copy Editor:
Pei-Yun Wang
Production Editor:
Pei-Yun Wang

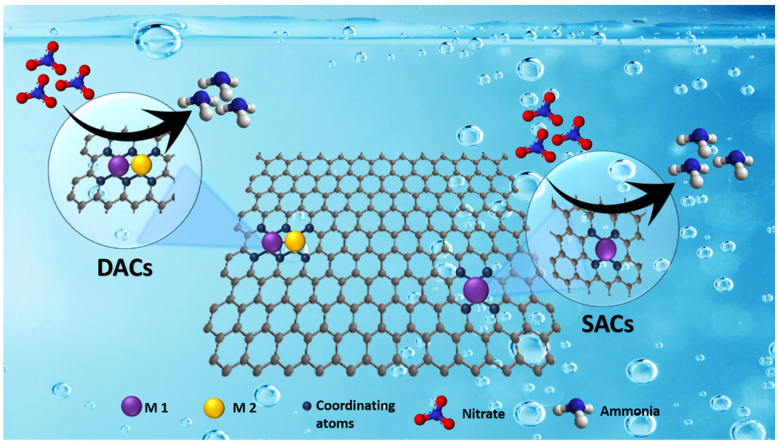

Abstract

Ammonia is a leading chemical in the agriculture, industry, and energy sectors, whereas nitrates are undesirable pollutants with harmful effects on the environment. Nitrate reduction to ammonia offers an efficient and sustainable route to produce green ammonia from waste nitrates. In this context, single- and dual-atom catalysts are considered the most promising owing to their maximum atomic utilization, highly tunable electronic structure, and well-defined active sites. This review focuses on the mechanism of nitrate reduction on single- and dual-atom catalysts, critically discussing the choice of metal, the engineering of coordination environment, and the effects of heteroatom doping. It also elaborates key performance descriptors and relates them to catalyst structure; the influence of operating parameters is also shown to be critical in determining catalytic activity and selectivity. The review further discusses how density functional theory and

[1]Catalysis and Surface Chemistry Laboratory, Department of Chemistry, School of Natural Sciences, National University of Sciences and Technology (NUST), Islamabad 44000, Pakistan.
[2]College of Intelligent Manufacturing and Mechanical Engineering, Hunan Institute of Technology, Hengyang 421002, Hunan, China.
[3]Institute of Chemistry, The Islamia University of Bahawalpur, Bahawalpur 63100, Pakistan.
[4]Tianjin Key Laboratory for Rare Earth Materials and Applications, School of Materials Science and Engineering, Nankai University, Tianjin 300350, China.
[5]Institute for Advanced Study, Shenzhen University, Shenzhen 518060, Guangdong, China.
[6]Shimmer Center, Tianfu Jiangxi Laboratory, Chengdu 641419, Sichuan, China.

*Correspondence to: Dr. Syed Shoaib Ahmad Shah, Catalysis and Surface Chemistry Laboratory, Department of Chemistry, School of Natural Sciences, National University of Sciences and Technology (NUST), Islamabad 44000, Pakistan. E-mail: shoaib.ahmad@sns.nust.edu.pk; Prof. Pengcheng Guo, College of Intelligent Manufacturing and Mechanical Engineering, Hunan Institute of Technology, Hengyang 421002, Hunan, China. E-mail: 2024001005@hnit.edu.cn; Prof. Xingke Cai, Institute for Advanced Study, Shenzhen University, Shenzhen 518060, Guangdong, China. E-mail: cai.xingke@szu.edu.cn; Dr. Tayyaba Najam, Institute of Chemistry, The Islamia University of Bahawalpur, Bahawalpur 63100, Pakistan. E-mail: tayyabnajam@szu.edu.cn

computational studies aid in the design and understanding of the operation of such catalysts. Finally, challenges and future research directions are elaborated to set a roadmap for researchers in the field.

INTRODUCTION

Ammonia is a key player in the agriculture and energy sectors, being a precursor and feedstock of fertilizers, and a clean and high energy density fuel[1-3]. It is equally important in the industrial manufacture of chemicals such as hydrazine, explosives, and synthetic fibers, as a refrigerant, solvent and pH modulator in pharmaceutical products. Conventionally, it is produced by the Haber-Bosch process, which is not only energy intensive but also relies on fossil fuels, increasing the carbon footprint in the atmosphere[4]. Carbon-free electrochemical reduction of nitrates is an excellent alternative to the conventional ammonia synthesis method. Nitrates accumulate in water bodies through agricultural runoff and industrial discharge, making aquatic life and human health vulnerable. Nitrate reduction to ammonia (NRA) is a green, sustainable, circular-economy-based method, that converts nitrate pollutants into useful ammonia[5].

Different materials have been used as electrocatalysts for nitrate reduction, including metal-organic frameworks (MOFs)[6,7], metals and metal alloys[8,9], metal oxides[10,11], electrified membranes[12], various composites[13], single-atom catalysts (SACs) and dual-atom catalysts (DACs)[14,15]. SACs bridge heterogeneous and homogeneous catalysis by dispersing individual metal atoms on support materials[16,17]. They are known for their high atomic utilization, as each atomic center is exposed instead of being buried in bulk, making them economical, especially for precious metals. All metal atoms have well-defined coordination environments and uniform active sites, imparting high selectivity and enabling facile optimization of the coordination environment. Furthermore, when single atoms are coordinatively unsaturated, they exhibit high affinity and lower activation energies for reactant species, enhancing the activity of the catalyst[18-20]. These unique features make SACs outperforming in various electrochemical reactions[21-25].

DAC is another advanced catalyst, sometimes referred to as a binuclear or diatomic catalyst. In DACs, two individual (same or different) metal atoms are coupled together as active sites, and scattered on the support material, similar to SACs[26]. They offer dimeric active sites with synergistic mechanisms on both atoms, allowing the simultaneous adsorption and stabilization of multiple reaction intermediates. Different metal combinations create unique electronic structures with tunable properties, enhancing the reactivity, selectivity, and catalytic efficiency of DACs[26-29]. These properties make them superior to SACs in many aspects, multi-electron reactions, where synergistic mechanisms on both metal sites are advantageous over individually scattered atoms[28,30,31].

Numerous SACs and DACs have been reported for NRA. Though both are challenging to synthesize, yet they outperform other catalysts in Faradaic efficiency (FE), yield rate, and atomic utilization. SACs for NRA have been reviewed extensively, focusing on synthesis, microenvironment tuning, effects of the support material, and reaction mechanisms, and listing transition metal SACs for NRA[32-35]. To the best of our knowledge, no review has provided a comparative analysis of SACs and DACs for NRA along with insights into DAC mechanism. DACs for NRA are growing rapidly, and a comprehensive review is needed not only to list all DACs but also to provide critical analysis and theoretical details in parallel with SACs. Our review provides mechanistic details of NRA on SACs and DACs, discussing the effects of different metals and metal combinations, microenvironments, their symmetry and saturation, performance parameters and descriptors, as well as density functional theory (DFT) screening of different catalysts, concluding with challenges in the field and a future roadmap for researchers. A comparison of SACs and DACs is summarized in Figure 1.

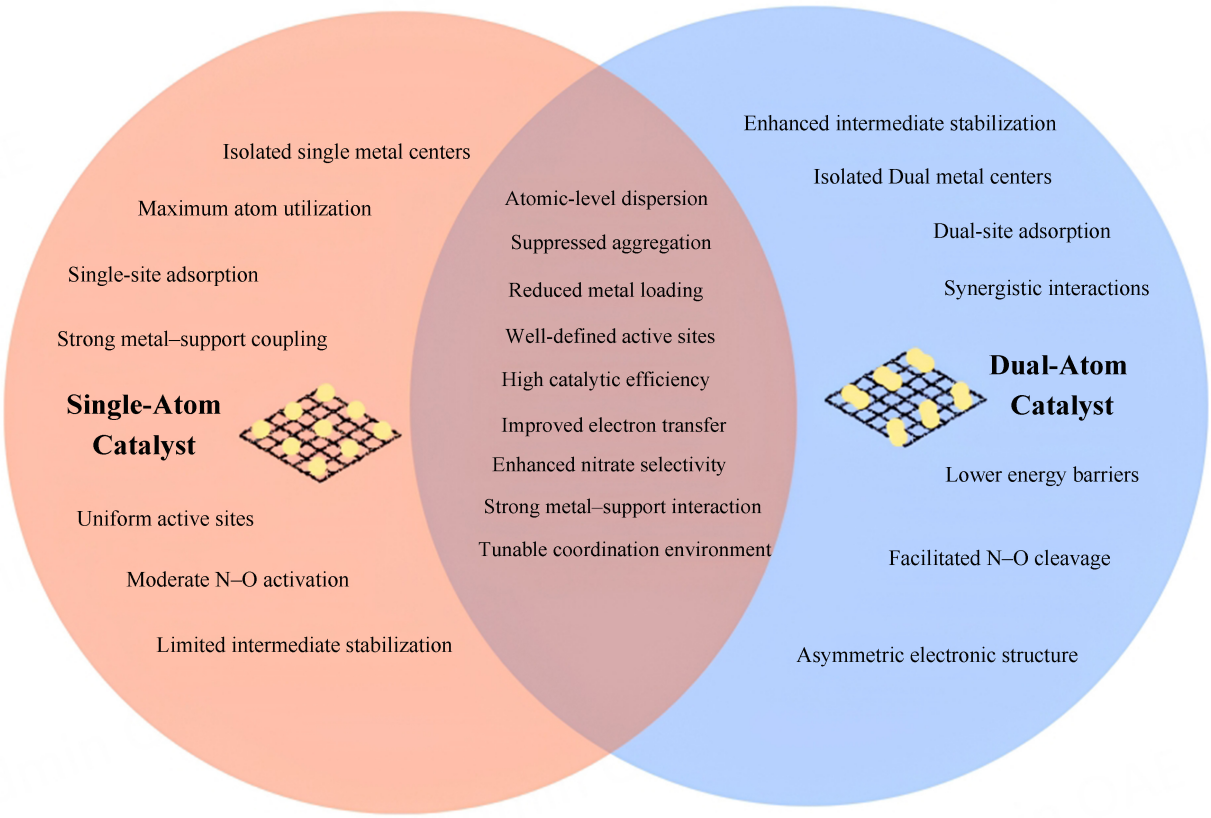

Figure 1. SACs and DACs comparison. SACs: Single-atom catalysts; DACs: dual-atom catalysts.

REACTION MECHANISMS AND PATHWAYS

NRA is a multistep electrochemical process involving eight electrons and nine protons as hydrogen source. Understanding the reaction pathways, intermediates formed, and their kinetics is crucial for the logical design of efficient SACs. The general mechanism includes a series of deoxygenation steps followed by hydrogenation steps, involving six intermediates and finally yielding NH_3 and aqueous NH_4^+. Each step involves proton-coupled electron transfer (PCET), which means that both proton and electron are transferred to the absorbed intermediate to drive the reaction forward[36].

$$NO_3^- \text{ (aqueous)} \rightarrow {}^*NO_3 \rightarrow {}^*NO_2 \rightarrow {}^*NO \rightarrow {}^*NOH \rightarrow {}^*N \rightarrow {}^*NH \rightarrow {}^*NH_2 \rightarrow {}^*NH_3 \rightarrow NH_4^+ \text{ (aqueous)}$$

Usually, first step is the rate-determining step (RDS), but this may vary depending on the SAC, the support materials, the coordination environment of the SAC, and the reaction conditions[37-39].

Mechanism on SAC

SACs feature atomically dispersed and completely separated metal centers on a support material, with the ability to finely optimize the adsorption of intermediates on the catalyst as well as their activation. The catalytic sites are inherently separated in SACs, which makes them effective in minimizing unwanted coupling products such as N_2 and N_2O. By preventing such coupling reactions, sequential hydrogenation dominates, boosting the selectivity of SACs for ammonia[32,38].

The overall kinetics of NRA is determined by the activation energies of individual steps and the stability of the intermediates. To optimize catalysts, it is necessary to determine the RDS. The formation of NO_2 is often

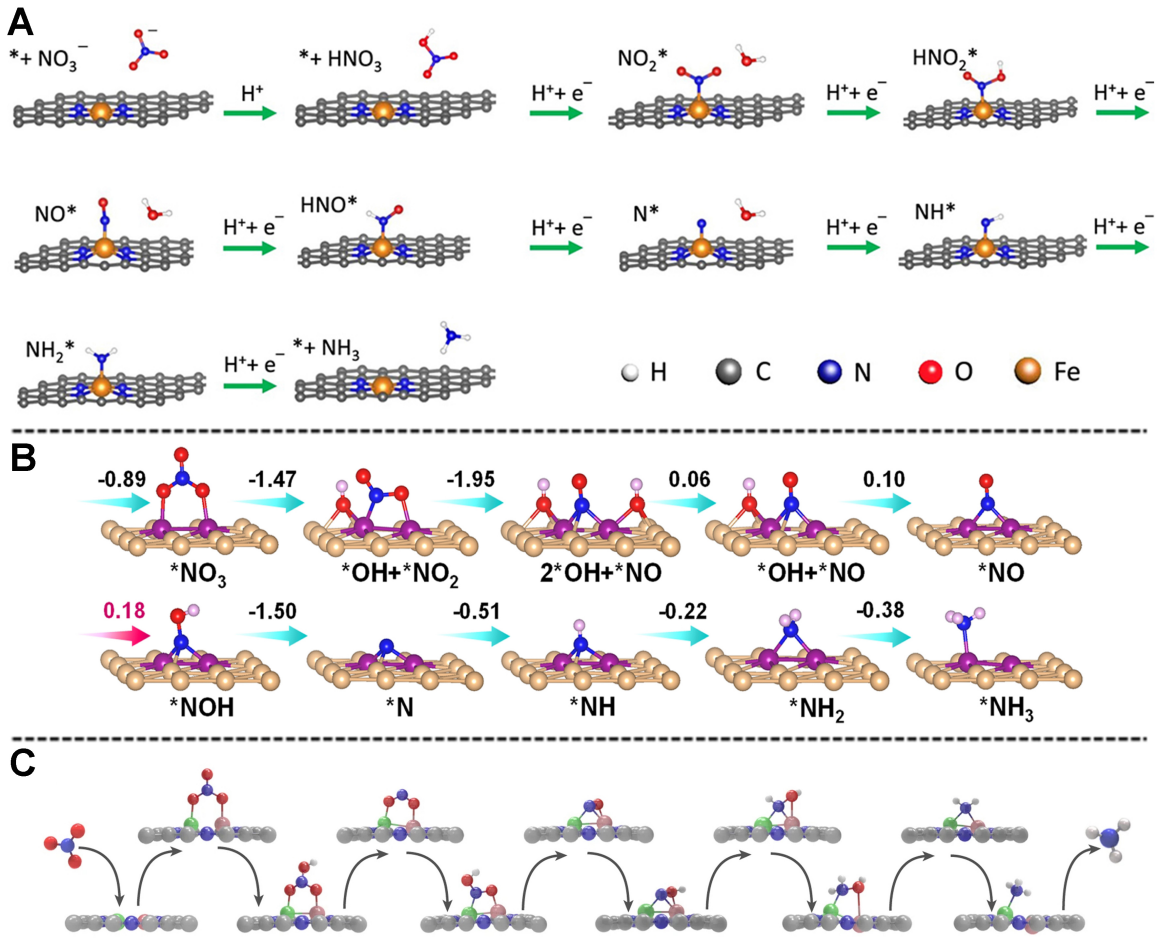

Figure 2. (A) Optimized geometries of the NRA intermediates for each step of the Fe SAC. License under a Creative Commons CC BY 4.0, from Ref.[40]; (B) Optimized geometries of the NRA intermediates for each step of the Cu-Cu DAC (purple: Cu, Blue: nitrogen, Red: Oxygen, light pink: hydrogen). Reproduced with permission from Ref.[46], Copyright 2024 RSC; (C) Optimized geometries of the NRA intermediates for each elementary step of the Fe-Cu DAC (Green: Fe, Pink: Cu, Blue: nitrogen, Red: Oxygen, white: hydrogen). License under a Creative Commons CC BY 4.0, from Ref.[51]. NRA: Nitrate reduction to ammonia; SAC: single-atom catalyst; DAC: dual-atom catalyst.

considered to be the RDS because of high dissociation energy of the N–O bond in NO_3; for other catalysts, NOH limits the formation of NH_3 because of a high energy barrier to form N* and side reactions into N_2. Figure 2A shows how nitrate is reduced to ammonia on the surface of a Fe SAC[37,40]. The adsorption energies of intermediates also play a critical role, as strong binding leads to catalyst poisoning, while weak binding results in desorption and a decrease in activity[41]. NO* is a critical intermediate situated at the crossroads of two reactions; a low desorption energy causes it to desorb as a gas and/or couple to form N_2 or N_2O, whereas strong adsorption promotes sequential hydrogenation to produce NH_3[42].

The competitive hydrogen evolution reaction (HER) is another significant challenge in NRA, as it consumes protons and electrons, reducing ammonia production and hence FE[43]. SACs are superior to other catalysts in mitigating HER by tuning the binding energies of intermediates. They make the adsorption of intermediates more favorable than hydrogen absorption, thereby reducing H_2 product[37,44]. Because it is difficult to extract and characterize intermediates and to experimentally verify the mechanisms; therefore, researchers rely on DFT calculations to elaborate how the catalyst works[45].

Mechanism on DAC

The fundamental reaction path and key intermediates for DACs are similar to those of SACs. However, the mechanism of individual steps is fundamentally altered owing to the presence of two adjacent active sites. These two sites perform distinct functions, making the catalytic process more efficient through a division of labor. DACs are more efficient in stabilizing intermediates because of the dual active sites, which directly or indirectly alter the electronic environment and improve the performance matrix of the catalyst for NRA. In SACs, only one active site is present, which must both stabilize the intermediates and supply hydrogen. These two functions cannot be performed efficiently and simultaneously at a single site. Therefore, the reaction faces higher energy barriers and proceeds more slowly than on DACs, where the bifunctional active sites work synergistically. Wang *et al.* designed a dual Cu atom catalyst, where both Cu atoms stabilize the NO_x-intermediates by forming bridged species, as represented in Figure 2B[46]. This makes DACs superior catalysts in terms of intermediate stabilization and faster reaction kinetics.

The two atoms may work synergistically, where one adsorbs nitrate and the other is responsible for water activation to provide H^+ for hydrogenation. Chen *et al.* reported a dipole coupled Cu-Pd DAC, in which Pd being more electronegative than Cu, generates and provides H* to Cu, while Cu itself is responsible for adsorbing NO_2^-[47]. Tandem catalysis is another mechanism followed by DACs, where one metal atom carries out the initial steps of NRA and further reduction is completed by another active site. Wan *et al.* synthesized a Mo-Fe DAC for NRA, where Mo converts NO_3^- to NO_2^-, which is then desorbed from the active site[48]. The Fe atom, serving as the second active site, adsorb the NO_2^- and complete its reduction to NH_3. Xiao *et al.* developed a frustrated Lewis pair (FLP) DAC for NRA, where Cu adsorbs and reduces NO_3^- to NO_2^-, as its d orbital is close to the π^* lowest unoccupied molecular orbital (LUMO) of NO_3^-, while Co was found to be suitable for NO_2^- as its d orbital matches to the π^* LUMO of NO_2^-[49]. This DAC showed faster kinetics and 100% FE, whereas in a SAC, intermediates accumulate leading to a lower FE.

In DACs, shared electrons are present owing to metal-metal interactions; therefore, they can easily donate electrons during the reduction process, lowering the overpotentials for each reduction step. In contrast, SACs require higher overpotentials to complete the same reduction steps because of limited electron availability. Chen *et al.* reported that a Pd-Cu DAC exhibited a lower free energy (0.35 eV) than that of a Cu SAC (0.5 eV) because the electrons from both metals facilitate the reduction in the DAC[47]. Similarly, Xu *et al.* prepared a Co-Cu DAC which showed Gibbs free energy lower than those of Co and Cu SACs[50]. The Co-Cu DAC also showed lower potential of 0.12 V at the potential-determining step of NO* to HNO*, as one metal stabilizes NO* while the other provides H* for hydrogenation.

DACs can bind intermediates in diverse ways, either through N or O or both, forming bidentate structures. Zhang *et al.* reported Fe-Cu DACs with a detailed mechanism based on DFT and d orbital energies, and their studies elaborated how heteroatom DACs favor NRA by allowing intermediates to bind and adsorb on both atoms [Figure 2C][51]. The intermediates are stabilized by the dual active sites; thus, compared with SACs, coupling reactions and accumulated intermediates are better controlled[52].

DACs offer greater flexibility for tuning and optimizing NRA activity. Researchers are exploring different combinations of metals for different steps or for better stabilization of intermediates, whereas such versatility is lacking in SACs. In NRA, most intermediates are unstable, and mechanistic details for both SACs and DACs are obtained from DFT studies. In such studies, real experimental conditions such as the electrochemical environment, pH effects, and solvent interferences are not fully considered. The actual pathways may therefore vary, and researchers need to improve computational models to make them more reliable or provide experimental proof of the proposed pathways. Under applied potentials during NRA, SACs/DACs may undergo electrochemical changes: atoms may aggregate into clusters, migrate, or undergo

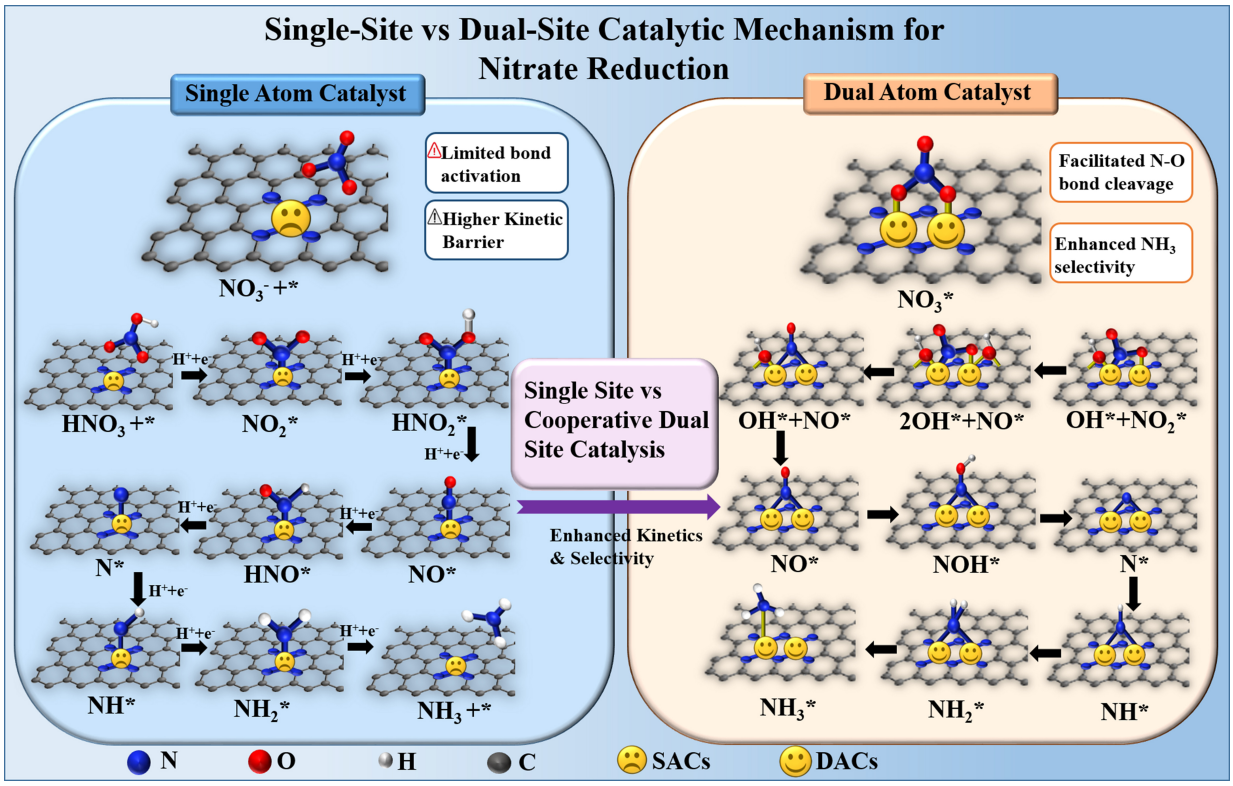

Figure 3. Comparative mechanism of nitrate reduction at SAC and DAC. SAC: Single-atom catalyst; DAC: dual-atom catalyst.

interatomic changes, all of which can alter the mechanism details. Therefore, post-NRA analysis and characterization are recommended for researchers in the field.

The supporting material and coordination environment determine the mechanism and the rate-limiting step, the pH of the electrolyte is particularly important in governing the NRA activity and stability of the catalyst. More studies are needed to determine the interrelations among these factors. Most researchers have compared SACs and DACs in terms of activity and FE but have not compared them with state-of-the-art catalysts[53,54].

To sum up, the mechanism details of SACs/DACs rely on computational studies and lack experimental validation. DFT efficiently depicts SACs as operating via Langmuir-Hinshelwood pathways by mapping potential energy surfaces, while most DACs feature bifunctional sites, with one focused on N-species and the other on PCET. These computational models typically treat catalysts as having perfect structures, ignoring *in-situ* reconstruction, the interaction of various components, electrolyte effects, and competition for adsorption sites. Similarly, for DACs, the migration of intermediates between dual atoms is not thoroughly understood. There is currently no method to validate that the increased activity results from the synergistic effects of dual metal sites rather from two separate metal sites that do not interact effectively. Operando electrochemical studies, isotopic labeling, Tafel slope analysis, and product formation are required to support DFT calculations. Time-resolved and surface-enhanced operando characterizations can help demonstrate that the DACs works synergistically as dual sites, rather than as two independent single sites. A mechanistic comparison of NRA on SACs and DACs is presented in Figure 3, showing the facilitation of NRA on DAC owing to the presence of two metal centers.

ROLE OF METALS

SACs can achieve 100% exposure of active sites, representing the theoretical limit of atom utilization, with highly tunable electronic structures, allowing for fine optimization of reaction mechanisms. Different metals offer different strengths for NRA. For example, Cu is the only non-noble metal with a d orbital energy close to the LUMO of nitrates. Cu (I) adsorbs nitrates more strongly than Cu (II). Cu SAC has been reported as the best performing SAC among Ni, Cu, Mn, Pd, Pt, Ru and Ga on nitrogen-doped carbon (NC), with 100% FE and a yield rate of 32,300 $\mu g \cdot h^{-1} \cdot mg_{cat}^{-1}$. Fe binds through oxygen, offering high selectivity for ammonia and stability over a wide pH range. Iron is used in NRA because of its natural role in nitrogen fixation to ammonia by the nitrogenase enzymes of nitrogen-fixing bacteria[40,55]. Cobalt is known for its ability to enhance the N–O bond cleavage, favoring ammonia formation over nitrogen gas. Co is known for its poor HER activity, but doping with noble metals provides sufficient HER happen to promote the reduction of nitrates to ammonia without lowering the FE[56,57]. Os is known for its low limiting potential of -0.42 V, as calculated by Wang *et al.* using a four-step screening high-throughput first-principle, highlighting the strong binding of Os with the oxygen of NO_3^- due to rapid charge transfer from Os to NO_3^-[58]. Shang *et al.* reported a Ru SAC in coordination with Bi for the efficient reduction of NO_2^-, with a FE towards ammonia[59]. This suggests the use of Ru in DACs for NRA to adsorb intermediates and conduct tandem reduction after NO_2^- formation.

Similarly, the choice of metals in DACs is also important, and DACs can be homonuclear or heteronuclear. In homonuclear DACs, both metal atoms are identical. They offer well-defined symmetry in the active sites, enabling a better understanding of metal-metal interactions and their effects on NRA activity. Mechanistic understanding of homo-DACs is easy because of symmetric charge distribution and uniform active sites, which facilitates the optimization of catalytic activity[60-62]. Pandiyan and co-worker computationally screened five DACs, all of which showed high FE reaching 100% for Rh-Rh at low limiting potentials ranging from -0.16 to -0.4 V *vs.* RHE. For the calculations, spin-polarized DFT was run using the Vienna ab initio simulation package (VASP)[63]. In heteronuclear DACs, each metal overcomes the limitations of the other, and synergistic working optimizes the NRA performance of the catalyst. Heteronuclear DACs are more competitive because of their bifunctional active sites, which may offer a tandem mechanism. Both metals may belong to the 3d series, or one may belong to higher d series; combinations of only higher d series for NRA are less common. Asymmetric electronic distribution and non-uniform active sites with strong d-d interactions generate molecule-like electronic states near Fermi level, giving rise to a donor–acceptor mechanism. This makes the origin of catalytic activity less predictable, and therefore their optimization is comparatively more challenging than that of homo-DACs[64]. Zhao *et al.* screened several metal atoms through calculation to identify the best heteroatom to form a DAC with Cu, based on NO_3^- adsorption energy, and free energy changes for $OH^* + H^+ + e^- \rightarrow H_2O$[45]. The results indicated that Fe, Pt, Ir, and Mn are promising. Additionally, it has been reported that Cu–Pd DAC have been applied for NRA, where Cu performs well in oxygen addition but is insufficient in hydrogenation[47]. Introducing Pd as an active site can enhance the supply of atomic hydrogen H* by promoting water dissociation. Zhang *et al.* showed that a Pd-Cu DAC exhibits a higher ammonia yield rate than Pd SAC and Cu SAC at lower potentials of -0.1 and -0.2 V *vs.* reversible hydrogen electrode (RHE)[65]. In a Fe-Mo DAC, Mo is chosen based upon its activity in nitrogenase, while Fe works to lower the thermodynamics barriers for NRA. Through their synergistic coupling, this catalyst achieves an ammonia yield rate of 13.56 $mg \cdot cm^{-2} \cdot h^{-1}$ and a FE as high as 94%, outperforming the respective SACs of Fe and Mo[48]. Cu-Co DACs have also been reported as a successful couple in multiple coordination environments, with an ammonia yield of up to 482.56 $mmol \cdot g^{-1} \cdot h^{-1}$, maintaining performance for 150 h without significant activity loss. DACs with Co doping have shown promising DFT-backed results, but experimental verification is still required[49,50]. Zhang *et al.* reported a Cu-Fe DAC on nitrogen-doped graphene which achieves a FE of 92.51% at a low potential of just -0.3 V *vs.* RHE[51]. The study shows that the dual active sites form by coupling Fe with Cu facilitate the adsorption and

discharge of nitrate ions, weakening the N–O bond and lowering the overall energy barrier of NRA. Additionally, Meng *et al.* further designed the same Fe-Cu DAC supported on NC as a selective catalyst for NRA, delivering a FE of 95% and a yield rate of 6.13 $mg \cdot h^{-1} \cdot mg_{cat}^{-1}$[66]. This DAC prevents the desorption of NO_2^- and other intermediates, shifting the reaction toward NRA and mitigating the accumulation of intermediates. In SACs, NO_3^- binds to the metal through O, while NO_2^- binds through N; thus, desorption is mandatory for the reaction to proceed. In DACs, when the two metal atoms are in proximity, NO_2^- does not need to desorb, but can simply shift to the adjacent atom, thereby skipping the desorption step and improving the FE[67]. Liu *et al.* also prepared an asymmetric Ru-Cu DAC, achieving a FE of 95.7% at 0.4 V *vs.* RHE[52]. Both studies have demonstrated the potential of Ru in DACs for NRA. Wei *et al.* prepared DAC combining Zn with various metals (Co, Fe, Mn, Pd, Pt, Ni, Ru) using a MOF as the precursor[68]. Among them, the Zn-Co DAC with an asymmetric coordination environment stands out, achieving a FE of 98.95% for NRA at -0.4 V *vs.* RHE and maintaining this efficiency over seven consecutive cycles. A Ni-Co DAC on MXene has been reported with a FE toward NH_3 higher than Ni and Co SACs, reaching a maximum of 92.46% with minor changes over ten cycles. Here, both metals act synergistically by coupling electron interactions; empty d orbital attract NO_3^-, while occupied ones donate electrons for the reduction of NO_x species[69]. Therefore, one site facilitates NO_3^- attraction and adsorption, and the other favors reduction of NO_x, leading to NH_3 production even at a low potential of -0.37 V *vs.* RHE. Feng *et al.* designed a metal-free DAC with Si and iodine on a Ni-O film, where iodine modified the electronic structure, promoting H* availability for nitrate reduction, while Si stabilized the catalyst, preventing the leaching of Ni from the supporting film[70]. This opens another potential option for making DACs that are metal-free and more stable than the metal DACs. Shen *et al.* reported a Cu-WO_3 DAC for NRA, showing that the electron deficient structure of the synthesized DAC promotes nitrate adsorption and facilitates the dissociation of H_2O for supplying H*[71]. Metal oxides are similar to metals in oxygen coordination environments, where oxygen optimizes the nitration reduction abilities. Ren *et al.* introduced a new direction by actively participating in support so that the single-atom and a support atom function as DACs[72]. They anchored a Cu SAC on NiFe layer double hydroxide (LDH) using a special cation vacancy generation method, which modulated the adsorption and surface accumulation of intermediates, as well as the availability of H*. This results in a high FE of 92% and an ammonia yield of 2.08 $mg \cdot cm^{-2} \cdot h^{-1}$. A Cu-Ru DAC has also been reported as one of the highest performing catalysts for NRA, showing maintained activity for 108 h[52]. It worked in both neutral and alkaline media, giving ammonia yield rates from 35.44 to 125.44 $mg \cdot h^{-1} \cdot cm^{-2}$ with a FE above 90%.

Computational studies, together with the experimental work, showed that the central metal in SAC and the metal combinations in DAC are not sole determining factors for NRA[73]. The coordination environment, support material, and interaction of metals with these are also of prime importance, as the same metals can exhibit different activities in different coordination environments and on different supports. Os SACs were found to be the best in terms of FE and yield on nitrogen-doped graphene, whereas Ru SAC outperformed when the support material was a graphitic carbon nitride framework. This suggests that the interactions of the metal(s) with the surrounding coordination environment determine the NRA activity of catalysts[32]. Oxyphilic metals like Cr, Mn, Fe, Ru form O-M-N_4 via oxygenation upon exposure to nitrate ions, while Co, Ni, Cu, Pd, and La sites run associative adsorption of NO_3^- to produce ammonia proceeding through NO_2 intermediates[74].

The choice of metal in SACs/DACs presents the thermodynamic limits of NRA. Every metal has some limitations in SACs. For instance, Cu d-orbital is close to the LUMO of nitrate, but it delivers incomplete reduction; similarly, Fe binds nitrate so strongly that desorption is tough, leading to catalyst poisoning. DACs are better in this regard, as they use two metals to overcome these limitations, yet other critical gaps remain. Both metals may compete for the same reactants/intermediates, causing them to interfere with each other.

The main challenges for SACs/DACs lie in their stability during electrolysis. Aggregation, clustering, and leaching of metal are prevalent, causing the catalytic activity to decline with increasing cycle numbers. Moreover, all work on SACs/DACs remain at the laboratory scale; to advance them toward practical applications, scalable production and field testing are required. Computer screening is being used in designing SACs/DACs, and the use of artificial intelligence and machine learning is strongly recommended to achieve better designs, provided that all experimental factors are considered in the simulations. Triple metal atom catalysts represent another promising future direction worth exploring, yet their synthesis is more challenging[75]. Additionally, stimulus responsive SACs/DACs can also be designed to alter their coordination in response to the concentration of intermediates in the medium, thereby thermodynamically and kinetically favoring specific reduction steps[76].

COORDINATION ENVIRONMENT

The coordination environment is equally critical, influencing the electronic structure of active sites, the binding abilities, the stabilization of intermediates, and the overall catalysis mechanism. SACs/DACs provide exemplary precision in optimizing catalytic behavior through atomic level regulation of the coordination environment[54,77]. In multistep NRA, several key intermediates are involved. They bind to active sites through different atoms, requiring different potentials and energies for each step. This makes the optimum adsorption of all intermediates on the same active site a challenge, that can be met by a delicate balance of the coordination environment. The coordination environment is a multilayer framework that drives the electrolytic performance of SACs and DACs. In addition to atom directly bonded to the SACs/DACs, three other structural features are important: (1) the symmetry and asymmetry of the coordination environment; which controls the distribution of electron density at the active sites; (2) the saturation or unsaturation of the metal coordination; which determines the number of available active sites and the Lewis acidity; (3) the second shell coordinating heteroatom (not directly bonded to SACs/DACs), which operates through long range electronic and electrostatic interactions[78,79].

The type of first-shell coordinating atom directly regulates the electronic properties and the interaction of SACs with the reaction intermediates.

(i) M-N_x coordination: Many efficient SACs have been reported with central metal directly linked to N and supported on a carbon material. Zhao *et al.* designed a Cu-N_4 SAC supported on porous carbon, exhibiting a Faradaic efficiency of 87.2% and an ammonia selectivity of 94.1%, both of which are higher than those of Cu nanoparticles on the same substrate[80]. The nitrogen coordination environment in Cu-N_4 favors the hydrogenation of NO*, leading to high ammonia selectivity over N_2. This N-Metal bonding also stabilizes the SAC, fine-tunes its d-orbital, and improves the absorption of the reaction intermediates.

(ii) M-O_x coordination: Oxygen can also play a role for NRA but it is less commonly used. Sun *et al.* synthesized Mn-$(O\text{-}C_2)_4$ from bacterial cellulose, which showed a FE of 89% at -0.5 V *vs.* RHE[54]. In this catalyst, the oxygen coordination tunes the d orbitals of Mn atom, improving its interaction with the intermediates.

(iii) Mixed Ligand Environments: These involve two different atoms, coordinated to the metals. They further refine the electronic structures and the interactions with nitrate and other intermediates. Chen *et al.* reported a Fe SAC derived from ZIF-67 with sulfur coordination[81]. The sulfur modification makes the coordination asymmetric, enhancing the adsorption of NO_3^-, and achieving a FE of 93.9% at a lower potential of -0.47 V *vs.* RHE. This demonstrates how different bonding environments can impact the initial nitrate activation. Phosphorus bonded to the metals in CoCu DAC plays a critical role as part of the coordinating environment.

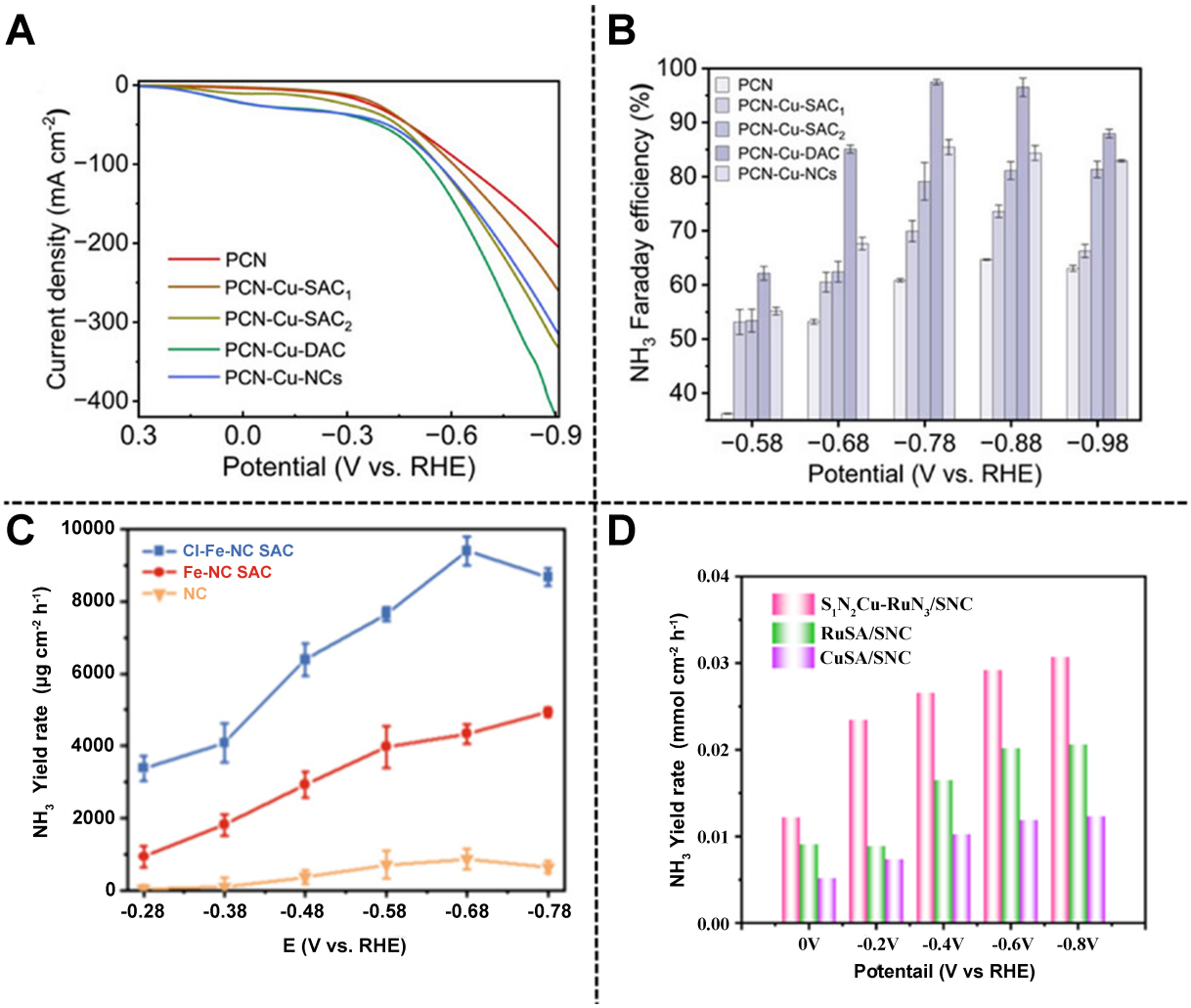

Figure 4. (A) LSV curves of PCN, PCN-Cu-SAC_1, PCN-Cu-SAC_2, PCN-Cu-DAC, and PCN-Cu-NCs in a mixed solution of 1 M KOH and 1 M KNO_3; (B) FE of the PCN, PCN-Cu-SAC_1, PCN-Cu-SAC_2, PCN-Cu-DAC, and PCN-Cu-NCs at different potentials for NRA in 1 M KNO_3 and 1 M KOH mixed solution reproduced with permission from Ref.[82] copyrights 2025 Wiley-VCH GmbH; (C) NH_3 yield rates at different applied potentials for Cl-Fe-NC SAC, Fe-NC SAC, and NC in a 1 M KOH electrolyte containing 0.1 M KNO_3 from axial chlorine reproduced with permission from Ref.[83] copyrights 2025 ACS; (D) NH_3 yield rates of N_2S_1Cu-RuN_3/SNC, RuSA/SNC, and CuSA/SNC reproduced with permission from Ref.[87] copyrights 2025 ACS. LSV: Linear sweep voltammetry; PCN: polymeric carbon nitride; SAC: single-atom catalyst; DAC: dual-atom catalyst; NCs: nitrogen-doped carbons; FE: Faradaic efficiency; NRA: nitrate reduction to ammonia; SNC: S, N co-doped carbon; RHE: reversible hydrogen electrode.

P changes the electronic density and facilitates charge transfer. It also helps to stabilize the intermediates that would otherwise poison the catalyst by blocking active sites. This DAC showed an ammonia yield of 1.59 mmol·h^{-1} and a FE of 95.36% at -0.3 V *vs.* RHE[50]. Li *et al.* designed an enzyme mimic DAC by anchoring Cu atoms on polymeric carbon nitride (PCN)[82]. PCN provides an enzyme-like coordination environment, making the Cu centers more positive, so that they efficiently attract NO_3^- ions. Consequently, this DAC showed the highest current in linear sweep voltammetry (LSV) and the highest FE among bare PCN, SAC PCN, and Cu- nanoparticles on PCN, as shown in Figure 4A and B.

Defects in the coordination environment promote nitrate reduction. Unsaturated sites favor the adsorption of NO_3^- and overall activity, the same holds true for an asymmetric coordination environment. Understanding how these defects interact: symmetric *vs.* asymmetric geometries, saturated *vs.* unsaturated coordination, and first *vs.* second-shell engineering enables the rational design of catalysts to achieve high FE and ammonia yield rates.

Researchers compared Cu SACs in different coordination symmetries with nitrogen and oxygen, like Cu-N_4, Cu-N_3, Cu-$2N_2O$ (cis and trans), through simulation-based studies for NRA. A study of radial distribution functions (RDFs) showed that cis Cu-$2N_2O$ exhibits the highest FE and absorbs the largest amount of nitrate ions on its surface[32]. The reason is that the cis geometry gives rise to local asymmetry, which in turn causes polarity in the structure. This polar structure attracts nitrate ions from electrolytes more strongly than other coordinating environments.

Wan *et al.* reported a Fe-N_4 SAC with axially coordinated Cl[83]. The axially attached chlorine atom modifies the electronic structure on Fe, stabilizing charge fluctuations at the active site. It increases the adsorption of NO_3^- and key intermediates, leading to a high FE of 99.4% at exceptionally low potential of -0.28 V *vs.* RHE, and showed a high ammonia yield in comparison to symmetric Fe-N_4, as shown in Figure 4C. Xue *et al.* compared a Cu SAC with N_4 and N_3C_1 coordination environment[84]. This work explains how breaking coordination symmetry creates spatial heterogeneity. The N_3C_1 configuration in Cu-N_3C_1 concentrates the charge density near Cu, leading to the adsorption of NO_3^- on Cu, while H* is absorbed on the nearby C. This adsorption behavior lowers the energy and makes the reduction reaction thermodynamically more favorable. This catalyst delivers a maximum FE of 94.8% and a stability of up to 84 h, both outperforming the symmetric Cu-N_4. Liu *et al.* prepared Cu SACs with different numbers of coordinating nitrogen: Cu-N_4, Cu-N_3, and Cu-N_2, and showed that Cu-N_4 better stabilizes the Cu active site, while Cu-N_2 is good at absorbing NO_2^-, thus preventing the accumulation of intermediates[85]. Hence, saturated and unsaturated coordination environments have different impacts on NRA activity.

The NRA activity of DACs is also affected by the coordination environment in similar patterns, with greater asymmetry and coupling caused by two metal atom sites. Lv *et al.* reported a Pd-Cu DAC embedded in asymmetric C_3N_4, the porous structure facilitates the incorporation of the metal atoms and lowers the Gibbs free energy and the limiting potential of the catalyst[15]. Cu-Co DACs with FLPs on NC showed relay kinetics and a push-pull mechanism for the adsorption and stabilization of NO_3^- and NO_2^-, forming Cu-O-N-O-N and Co-O-N-O structures in a nitrogen rich environment[49]. Wei *et al.* reported another Zn-Co DAC in an asymmetrical coordinated environment[68]. The metal-bonded nitrogen in the $N_3Zn–CoN_2$ configuration enhances the electronic coupling between the metal active sites, optimizes the adsorption of key intermediates especially NOH*, and reduces the energy required for the reduction reaction, thereby lowering the activation energy barrier.

Lian *et al.* reported an AgCu-C_3N_4 DAC, in which Cu acts as a Lewis acid through coordination with nitrogen to adsorb NO_3^- ions, while Ag, as a noble metal, promotes the supply of H*[86]. Under visible light irradiation, this DAC achieves an ammonia yield as high as 630.5 μmol·h^{-1}·g^{-1}. Yin *et al.* designed an N_2S_1Cu-RuN_3/SNC DAC featuring an asymmetrical coordinating environment and showing a FE of 98% at -0.6 V *vs.* RHE[87]. Sulfur plays a crucial role in modulating the electronic structure, facilitating intermediate adsorption and lowering the energy barrier. As shown in Figure 4D, the sulfur modified DAC shows higher FE and NH_3 yield than the same DAC without S.

Critical analysis of the coordination environment shows a significant gap between theoretical predictions and experimental results for SACs and DACs. Breaking symmetry is regarded as a strategy to increase activity, but there is no solid explanation confirming whether this enhancement arises from a change in coordination number or can be attributed to a change in the oxidation state of the metal. It demands more systematic studies and future research. Furthermore, current characterization methods cannot determine whether asymmetry, unsaturation, and other features of the coordination environment are merely spectators or real participants responsible for the activity. Without time-resolved operando techniques with atomic

resolution to capture coordination changes and the binding of intermediates during catalysis, the coordination-performance relationship remains more hypothetical than an established principle.

Second-shell heteroatom doping involves incorporating non-metal elements into the support material or the vicinity of active sites. These dopants alter the electronic structure of SACs modifying its catalytic performance, but they are not directly bonded to single metal atom. This approach is a transformative method for optimizing NRA activity. The dopant atoms are usually anchored on the support material (mostly carbon based), from where they modulate electronic structure by redistributing charge, strain engineering, and long-range electronic effects.

Chen *et al.* reported a P-doped Cu SAC in a nitrogen coordination environment; it lowered the energy barrier for the NO* to NOH* conversion, driving selectivity toward ammonia and increasing production rates[81]. P induces polarization in the structure, which strengths NO_3^- binding and drives H* supply, and an overall increase in current is observed[88]. Iodine as a dopant is known to alter adsorption preferences, favoring NO_3^- over H_2O/H*. Hence it suppresses HER competition and boosts ammonia yield[89]. Cai *et al.* reported an iodine doped Co SAC, formulated as CoN_4, which showed an ammonia yield rate of 18.64 $mg{\cdot}h^{-1}{\cdot}mg_{cat}^{-1}$ and high selectivity for NH_3 over H_2[90].

Doping in DACs is more complicated because of the interplay and constructive interaction of the two metal atoms, both of which may have different effects on the electronic structures of the dopants. Researchers reported boron doping on Ni-Co DAC; the boron favors the anchoring of Ni and Co on the carbon support and prevents the aggregation of metal atoms into clusters, which would otherwise decrease catalyst activity. Consequently, with B doping, a high NH_3 yield of 0.87 $mmol{\cdot}h^{-1}{\cdot}cm^{-2}$ at -0.3 V is achieved[91]. Selenium has also been found useful in enhancing the adsorption of NO* on Fe SAC, so it can be used for NRA as well, either alone or with another dopant[92]. The effect of dopants on NRA activity shows they are not merely a structural feature but an opportunity to fine-tune SACs/DACs for better performance.

SYNTHESIS METHODS AND STRUCTURE CORRELATION

Following the detailed discussion of SACs/DACs structural features, this section briefly examines synthesis methods, highlighting their pivotal role in achieving these specific structural features. While the synthesis techniques of SACs and DACs have been extensively reviewed by numerous researchers (Xiong *et al.*[93], Xiang *et al.*[37], Chao *et al.*[94] and Xu *et al.*[95]), the correlation between synthesis methods, structural features and NRA activity remained an underexplored area. This section provides an overview of the primary synthesis techniques, evaluating their influence on the resulting catalyst structure and their key role in NRA performance of SACs/DACs.

Pyrolysis

Pyrolysis is applied to synthesize SACs/DACs from MOFs, organic ligand-based compounds, and nitrogen rich precursors. Elevated temperature treatment (typically 600-1,000 °C) under inert atmosphere results in single or dual atoms, depending on the precursor anchored on porous carbon or N-doped porous carbon[39,96]. A Fe-Mo DAC was synthesized by Wan *et al.* via pyrolysis at 650 °C[48]. This method results in open porous structures with a large surface area, which facilitates mass transport and enhances catalytic activity through the adsorption of reactants and intermediates. Typically, this method generates a symmetric coordination environment, such as M-C or $M-N_4$, within carbon layers.

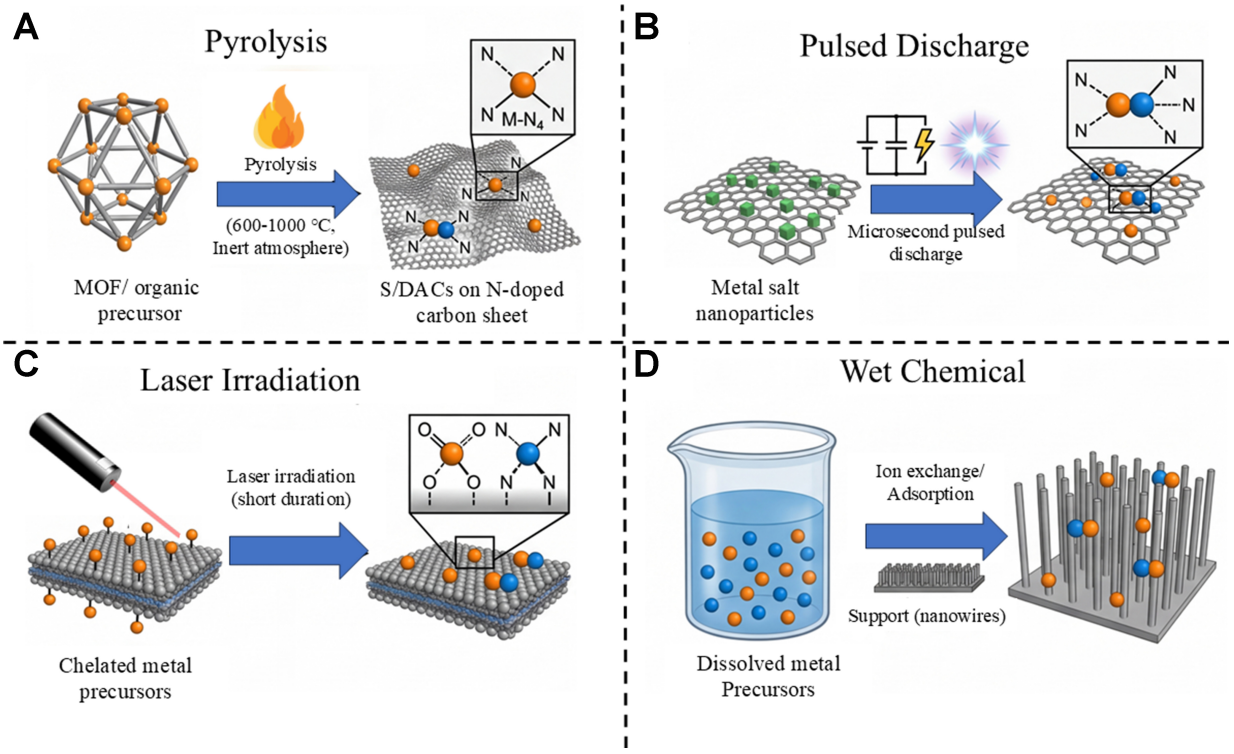

Figure 5. A schematic illustration of the synthesis strategies of SACs/DACs: (A) pyrolysis; (B) pulse discharge; (C) laser irradiation; (D) wet chemical. Each colour ball corresponds to metal atom, two different colours are used to show two different metals were involved. To show salt square shape was used in order to distinguish from metal atoms. SACs: Single-atom catalysts; DACs: dual-atom catalysts.

Pulsed discharge

Pulsed discharge is an advanced preparation method that utilizes microsecond high energy pulses for rapid generation of SACs and DACs. In this method, a pulsed discharge injects current into the metal source and CN precursors, resulting in instantaneous decomposition and atomic anchoring within microseconds[96]. Due to ultrafast heating and cooling, this method generates asymmetric structures, for example, RuN_2-CuN_3. This asymmetric coordination favors NRA by optimizing intermediates adsorption and lowering activation energies[52].

Laser-assisted synthesis

Laser irradiation is a low-energy, rapid, and scalable alternative to traditional pyrolysis. CO_2 laser beams or other laser waves are irradiated for a short duration on the metals chelated to the support materials, resulting in M–O and M–N bonds. This process provides high material transformation efficiency through heat diffusion[69,97,98]. Park *et al.* synthesized NiCo DACs on MXene using CO_2 laser irradiation for 10 min; the dual sites synergistically enhance NO_3^- adsorption and activation, outperforming their SACs[69].

Wet chemical methods

These methods are particularly useful when the precursors are in the liquid phase. They rely on surface chemistry and ion exchange principles to get atomic-level dispersion. Lian *et al.* reported Ag-Cu DACs for photocatalytic nitrate reduction prepared by ion exchange method[86]. Ag single atoms were anchored on Cu nanowires through ion exchange between $AgNO_3$ and $Cu(OH)_2$ nanowires. This method also presents a better alternative to pyrolysis in terms of energy input and time. These techniques, along with key points, have been summarized in Table 1 and illustrated in Figure 5.

Table 1. Summary of synthesis-performance relationships

Synthesis technique	Resulting structure	Performance characteristics
Pyrolysis	Atomically dispersed M-N_4 sites embedded in porous carbon/N-doped porous carbon	High porosity, high surface area, high mass transport
Pulsed discharge	Asymmetric coordination environments	Rapid synthesis, ultrafast temperature change preserves metastable, high-energy active sites
Laser irradiation	Single atoms anchored via M–O or M–N bonds on defect-rich conductive substrate	Rapid synthesis, low overall energy input, strong metal-support interaction
Wet chemical	Atomically dispersed metal sites anchored on conductive nanostructures	Improved dispersion, maximum atomic utilization

Defect engineering is a versatile strategy applicable to any SACs/DACs synthesis method. Defects such as vacancies, heteroatoms, and intrinsic defects in the coordination environment have proven useful in enhancing NRA activity[99].

DFT AND COMPUTATIONAL STUDIES

DFT and computational studies are indispensable in SACs/DACs research. Researchers employ DFT to support and elucidate experimental work and mechanisms, as well as to predict active metals under specific conditions.

Xue *et al.* used the VASP package along with the Perdew-Burke-Ernzerhof (PBE) exchange correlation functional for DFT calculations[100]. Bader analysis was used to quantify charge, and thermal stability was assessed by *ab initio* molecular dynamics. They identified a PdCu catalyst that is effective in preventing HER and selective for NH_3.

Lv *et al.* studied catalysts under a wide pH range using the CASTEP software package[15]. Projected density of states (PDOS) and surface Pourbaix diagrams were utilized to investigate electronic properties. Simulations predicted TiFe as the best-performing DAC among thirty-six combinations on the g-C_3N_4 surface. This provided a guide to identify optimal metal combinations for DACs.

Zhao *et al.* screened 80 transition metals using spin-polarized DFT and climbing-image nudged elastic band (CI-NEB) method[60]. A three-step screening approach was employed to study energy barriers, and Cu homonuclear dual atom on N-doped graphene was demonstrated to be the optimal candidate catalyst for NRA. Experimental studies validated the theoretical results, showing 97.4% FE for the catalyst at low potential of -0.14 V *vs.* RHE. This method can be employed to avoid trial-and-error preparation of SACs and DACs for NRA. Furthermore, Zhao *et al.* also used spin-polarized DFT to study dual heteroatom doping on CoP SAC, and performed *ab initio* molecular dynamics simulations at 300 K, thus revealing the bidentate bonding mode of intermediates and the bidirectional current flow initiated by the double heteroatom, which is expected to lay the foundation for the theoretical regulation of the microenvironment[67].

Wang *et al.* investigated 300 heteronuclear DACs by employing high-throughput first-principles calculations and a hierarchical four-step screening method[64]. To simulate varying electrochemical conditions, a constant-potential model was utilized. The results indicated that Cr-Rh and Mn-Rh exhibit high selectivity and activity at extremely low potentials of -0.16 and -0.25 V, respectively. Furthermore, it is confirmed that the orbital interaction of two metals produces activity under an association-dissociation mechanism. Wang *et al.* also employed DFT simulations along with PDOS analysis[101]. By coupling these calculations with *in-situ* Fourier-transform infrared spectroscopy and electron paramagnetic resonance reaction intermediates

Table 2. Recently designed SACs and DACs for NRA (all working potentials are against RHE)

SACs/DACs	Electrolyte	Support	Yield rate	FE %	Ref.
Cl-Fe-N_4	-	NC	9,396.7 $\mu g \cdot h^{-1} \cdot cm^{-2}$ at -0.68 V	99.4 at -0.28 V	[83]
Pd-Cu DAC	-		1.98 $mM \cdot h^{-1} \cdot cm^{-2}$ at -0.2 V	94.4	[47]
Cu-Co DAC	-	NC	482.56 $mmol \cdot g^{-1} \cdot h^{-1}$	96	[49]
CoP/Cu_3P	-	CN wrapped carbon black	1.59 $mmol \cdot h^{-1}$ at -0.3 V	96.35	[50]
N_2S_1Cu-RuN_3/SNC	1 M NaOH and 0.1 M $NaNO_3$	SNC nanosheet	0.02919 $mmol \cdot cm^{-2} \cdot h^{-1}$ at -0.6 V	98.2	[87]
Zn_1Co_1-NC	-	NC	-	98.95 at -0.4 V	[68]
AgCu-CN	-	CN	630.5 $\mu mol \cdot h^{-1} \cdot g^{-1}$ under visible light	> 98	[86]
PCN-Cu-DAC	-	Polymeric CN	467 $mg \cdot h^{-1} \cdot mg_{cat}^{-1}$ and 102 $mg \cdot h^{-1} \cdot cm^{-2}$	-	[82]
NiNC	Basic with 13 pH	NC	615.7 ± 176.5 $\mu mol \cdot h^{-1} \cdot cm^{-2}$ at -0.4 V	78	[102]
Cu-Fe DAC	1 M KOH and 0.1 M KNO_3	NC	6.0 $mg \cdot cm^{-2} \cdot h^{-1}$ at -0.53 V	94.3	[103]

SACs: Single-atom catalysts; DACs: dual-atom catalysts; NRA: nitrate reduction to ammonia; RHE: reversible hydrogen electrode; FE: Faradaic efficiency; NC: nitrogen-doped carbon; CN: carbon nitrite; SNC: S, N co-doped carbon; PCN: polymeric carbon nitride.

were identified. The experimental work verified computational results by exhibiting a high FE of 98% and successful implementation in Zn-NO_3 batteries. This method can be employed for all similar catalysts to get an in-depth, simulations-based understanding of the mechanism.

Li *et al.* used DFT to study solvation effects and dispersion correction to efficiently predict catalyst activity[62]. DMol3 spin-unrestricted DFT-Sol and DFT-D were used for these purposes, respectively. An Os dimer was found to be the most promising catalyst on the CN surface at low potential of -0.15 V *vs.* RHE. Considering solvent effects gives a more refined value for limiting potential.

DFT has become essential in SACs/DAC research, and many simulation packages are available. However, no single simulation suite can study all aspects of a catalyst. Furthermore, the computational cost of such studies is remarkably high, taking hours to weeks. This also necessitates specialized experts; a wet chemistry scientist or material engineer cannot operate this complex software without extensive learning and training. Machine learning approaches are increasingly necessary. Well-trained machine learning models with user-friendly interfaces are highly in demand. Data scientists, computational chemists, and material experts need to collaborate to develop models that can be easily employed by lab scientists for prediction and mechanistic studies without requiring in-depth computational expertise.

PERFORMANCE EVALUATION AND BENCHMARKING

Comprehensive performance data

Recent advances in SACs and DACs have demonstrated remarkable progress in electrocatalytic nitrate-to-ammonia conversion, with performance metrics spanning wide ranges depending on the catalyst composition, coordination environment, and operating conditions. Table 2 presents a summary of recent works in the field.

Performance trends across variables

NRA activity varies with metal centers, as discussed in Section "Mechanism on SAC". Studies on MOF-derived SACs for several metals: Mn (II), Fe (III), Co (II), Ni (II), Cu (II), Zn (II), Mo (II), showed that Cu SACs and Fe SACs exhibit higher ability to perform NRA compared to other metals[85,104]. Their high performance also correlates with several factors. (i) d-electron configuration: Metals with half-filled d orbital

typically show superior activity compared to those metals with empty or fully filled d orbital; (ii) Oxophilicity: Moderate oxophilicity helps to perform better; otherwise NO_3^- is either poorly adsorbed or bind strongly, thereby restricting NRA activity; (iii) Hydrogenation capability: Metals capable of PCET show better activity than others. If metals fail to dissociate H_2O to generate H*, less reduction to ammonia takes place.

In acidic, neutral and basic media, Fe SACs on NC exhibited Faradaic efficiencies of more than 80% across the entire pH range. However, competition with HER varies with pH, as suggested by DFT and experimental work. Generally: (a) alkaline media show the highest selectivity, but activity is less as protonation is slow; (b) neutral electrolytes offer a balance between activity and selectivity; and (c) acidic media exhibit higher NRA activity, but HER is also increased[53,104].

The NRA activity of SACs/DACs have been evaluated in electrolytes with NO_3^- concentrations ranging from 100 ppm to 0.5 M. Typically, the activity of NRA increases with concentration, which is attributed to enhanced mass transport to the electrolyte, improved selectivity over HER, and an overall increase in current density[105]. However, beyond a certain concentration, this enhancing effect becomes negligible or even absent entirely, because the number of active sites in SACs and DACs is limited as compared to state-of-the-art catalyst.

Structure-performance relationships

The performance and selectivity of metal atoms in SACs/DACs are determined by coordinating atoms, their number and symmetry, as well as by dopants that indirectly coordinate to the metal atoms, influencing the FE, selectivity, yield rates, and adsorption of NO_x^- species[105]. Breaking symmetry enhances catalytic performance; an unsaturated coordination number favors the adsorption of NO_3^- and intermediates; second-shell heteroatoms, in turn, alter the reaction mechanism by modifying the electronic structure.

Support materials also have an impact on NRA, as same SACs/DACs on different supports give variable performance. Carbon based supports are the most widely used: (a) N doped carbon provides N for coordination environment and also stabilizing the catalyst; (b) graphene and carbon nanotubes (CNTs) as support offer better conductivity and mass transport, and are used in $ZnNO_3$ batteries; and (c) carbon aerogels are also used as 3D materials but are less common than others. MOF derived materials have metal atoms coordinated to linker atoms[106]. As in UiO-66 derived SACs, Zr nodes are bonded to oxygen atoms of the carboxylate linker, creating an oxygen rich microenvironment, which is helpful in attracting NO_3^- and transferring protons. Polymeric materials like PCN are also used to create enzyme mimic systems.

Operating condition dependencies

Applied potential alters performance, showing a hill-type behavior[107]: an optimal balance of selectivity and current is achieved at moderate potentials of -0.4 to -0.7 V; higher selectivity with lower current is observed at low potentials up to -0.4 V; and increased activity but reduced selectivity occurs at potentials more negative than -0.8 V due to severe HER. Not only pH but also the nature and concentration of supporting electrolyte matter critically. Fine tuning the electrolyte composition and concentration using rational approaches increases the FE multiple times. Usually, the concentration is between 0.1 and 1 M, and the pH is maintained using a buffer. Salts with K^+ are preferred over Na^+ owing to their better mobility and conductivity[107,108]. Most studies have been conducted at room temperature (25 °C); elevated temperatures offer increased mass transport and kinetics rates, but selectivity is decreased and the catalyst is prone to thermal degradation.

Stability and durability

A decrease in NRA activity is observed due to degradation of catalyst. Common failure modes include metal atoms aggregation into nanoparticles, support material corrosion under oxidative medium, poisoning of active sites by side products or impurities from the electrolyte, structural reconstruction of active sites during electrolysis, and sometimes metal leaching[52].

Data comparability and standardization needs

Assessing catalyst efficiency, competitive side reactions, selectivity for NH_3, and catalyst stability remains challenging. Ammonia quantification is the biggest challenge: all methods, including Nessler's reagent method, indophenol blue method, and ion chromatography, are affected by pH, incubation time, sacrificial agents, and interfering substances[109]. To obtain reproducible results, comprehensive guidelines and standard protocols should be followed.

The Nessler's reagent method is fast, with detection limit comparable to that of the indophenol method, but it involves toxic mercury and is sensitive to metal ion interferents and pH of solutions. Adding a masking agent and performing measurements under controlled temperature within 10-30 min minimizes variations. The indophenol blue method is more selective, does not involve toxic Hg, and offers stable color development, but it is slow, taking almost 2 h for complete reaction. The best protocols to get reproducible and standardized results recommend keeping all reagents and incubated solutions in the dark, using fresh reagents, and carefully controlling the pH. In contrast, the ion chromatography is extremely sensitive, offers automated operation with excellent reproducibility, and can detect NO_3^-, NO_2^-, NH_4^+ simultaneously; however, the instrumental setup is expensive, it requires skilled operators, regular calibration of instruments, and proper selection of eluents. Baseline correction and careful sample solution preparation are critical protocols[110].

To confirm that the origin of ammonia is nitrate, and not any impurities or N from the support material or the catalyst, isotopic labeling is required. Isotopic labeling is intended to verify the purity of the $^{15}NO_3^-$ source, and to detect the $^{15}NH_3/^{15}NH_4^+$ produced via nuclear magnetic resonance and mass spectrometry[111,112].

Ammonia yield is reported using various units and normalizations; these inconsistencies make comparison challenging or even impossible. Some researchers report mass-normalized yield like $\mu g \cdot h^{-1} \cdot mg_{cat}^{-1}$, $mg \cdot h^{-1} \cdot mg_{cat}^{-1}$ or $mmol \cdot h^{-1} \cdot mg_{cat}^{-1}$. These units account for catalyst loading, but the total mass of metal loaded varies widely (0.1%-5% wt.). Therefore, to enable direct comparison, the active metal mass should be specified. Another way of reporting is area-normalized yield, e.g., $\mu g \cdot h^{-1} \cdot cm^{-2}$ or $mg \cdot h^{-1} \cdot cm^{-2}$, which is useful for electrode applications. To address issues with such units, both the total geometric area of the electrode and the electrochemically active surface area should be reported[63,103]. Furthermore, FE and partial current density should be reported along with ammonia yield rate.

Several types of electrochemical setups are used in NRA experiments, including the H-type cell, flow cell, membrane-free systems. Reporting all setup details is crucial for useful comparisons. H-type cells are commonly used but face issues of membrane resistance and mass transport limitations. The condition and size of membrane are also critical. Standard washing protocols must be followed to prevent membrane clogging, which can lower current flow. Flow cells allow operation at much higher current densities than H-type cells due to enhanced mass transport. Consequently, results of the same catalyst can vary between these two setups. Membrane free systems are also used, but they make the process more complicated by mixing anodic and cathodic reactions and products[48,113]. An overview of all performance descriptors has been presented in Figure 6.

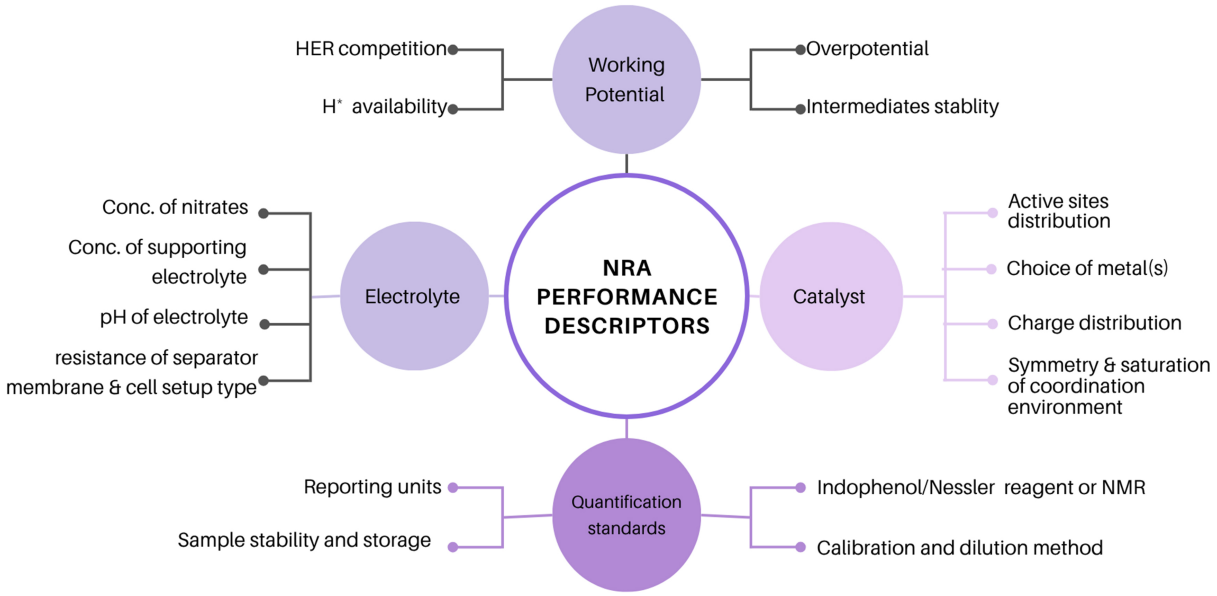

Figure 6. Overview of performance descriptors of NRA, elaborating role catalyst, electrolyte, working potential and quantification protocols. NRA: Nitrate reduction to ammonia; HER: hydrogen evolution reaction; NMR: nuclear magnetic resonance spectroscopy.

After reviewing SAC and DAC studies conducted under different reaction conditions are reported using different normalization methods, we strongly recommend establishing standard operating and reporting protocols for NRA. Such standardization would facilitate the comparison of catalytic activities and clarify the interrelationships among different influencing factors. The more comprehensive the reported data of a catalyst, the more useful it will be for the scientific community. Therefore, precise and detailed reporting is crucial for several aspects: catalyst characterizations (both before use and post-mortem, using the same techniques), electrochemical testing conditions, at least two independent quantification methods, isotopic labeling, *in-situ* and operando characterizations, minimum and maximum operating times, FE and yield rates (in both mass-normalized and area-normalized units), operating potentials, and standard reference conditions.

CHALLENGES AND FUTURE PERSPECTIVES

The greatest challenge lies in the precise preparation of SACs and DACs, with meticulous control over the coordination environment, dopant positioning, asymmetry, and unsaturation[114]. During catalysis process, the coordination environment is prone to change, which may cause migration, cluster or reorganization of ligands. Unsaturated sites may be saturated by adsorbing side products or intermediates. Furthermore, asymmetry and unsaturation in the coordinating environments, as well as specific heteroatom arrangement, are thermodynamically sensitive and less stable compared to saturated and symmetric systems. During electrolysis, the system tends to move toward higher stability at the expense of activity, resulting in a less active but more stable configuration. For instance, heteroatoms may migrate to energetically favorable positions, ligands may move to create a symmetrical coordination environment, or electrolyte species may bond on unsaturated sites[85].

Furthermore, it is difficult to determine whether the key tuning parameter for catalytic activity is the metal atom, the first-shell coordination geometry, the second-shell heteroatom, or even the reaction medium, including its pH and operating potential. Since tuning effects vary significantly and may even be contradictory across different cases, the contribution of all these features to the mechanism needs detailed discussion and evaluation to rationally optimize performance and design SACs/DACs. If a heteroatom or

vacancy concentration increases the activity, its optimum level and the interplay of other structural features need to be determined. It remains unexplored how different heteroatoms and coordination environments reinforce each other or act neutrally for NRA. This multilayered mapping of all parameters demands further studies[115,116].

Sometimes, during DAC preparation, one or two types of SACs are also formed. It is challenging to distinguish the NRA activity of SACs and DACs present on the same support. The mechanistic understanding of SACs/DACs is highly complicated; the intermediates are short-lived and often cannot be separated. Researchers rely on DFT, assisted by limited experimental data, to propose mechanisms. To date, DFT and computational screening do not offer a complete alternative of experimental work. Therefore, improved simulations and programs are needed that can consider not only structure of SACs/DACs but also all reaction parameters, such as pH, concentration of electrolyte, composition. *In-situ* and operando techniques are used for quantifications and mechanistic studies; however, these are extremely expensive and not universally available, thereby restricting research due to cost factors[62,103].

The absence of a standard framework for testing and reporting protocols severely restricts comparative studies and technology transfer. SACs/DACs are mostly tested under laboratory conditions. Their real-world field application and scaling present another significant challenge for researchers. A comprehensive cost and sustainability analysis is required to compare NRA using SACs/DACs with other technologies, assessing their real-world applicability and future potential.

SACs/DACs possess numerous structural details; each structural feature can be designed for specific steps of NRA. This systematic design approach will rationally optimize activity. For this purpose, a robust database needs to be designed, or machine learning models can be trained to correlate these structural features with reaction mechanisms, intermediate binding energies, and kinetics. Such models should be verified by experimental work. Utilizing such a trained and verified model, novel and unique combinations of metals, coordinating atoms, and dopants can be easily screened, and synergistic effects can be studied without the need for tedious synthesis. Machine learning can also be applied to inverse catalyst design. Instead of synthesizing SACs/DACs with features and then evaluating its performance computationally or experimentally, the focus should be on the potential of each step and the binding energies of intermediate. Subsequently, researchers can screen metal atoms and coordinating systems that can deliver the required features[117,118].

It is highly recommended to build universal metrics that quantify the extent of asymmetry, degree of unsaturation, and second shell coupling. This can be achieved by studying the dipole moment and symmetry order, the coordination number and Lewis acidity, and the strain energy, respectively. Such descriptors would make performance comparison possible across diverse catalyst families, enabling applications of design rules in general instead of specific systems.

Bioinspired catalysts for NRA are receiving growing attention, but further advances will require the incorporation of nitrate-reductase like coordination environments into synthetic catalysts and their optimization under realistic experimental conditions[82]. Similar to SACs and DACs, triple atom catalysts are also emerging, though they remain rare. There is a need to explore these for NRA and compare them with SACs/DACs. Multiple second shell dopants can also be incorporated to get various advantages[119].

Time-resolved X-ray spectroscopy with specific element detection can capture changes in first shell coordinated atoms and second shell dopants by utilizing extended X-ray absorption fine structure at both the metal K-edge and the dopant K-edge, respectively. If researchers combine this with electrochemical

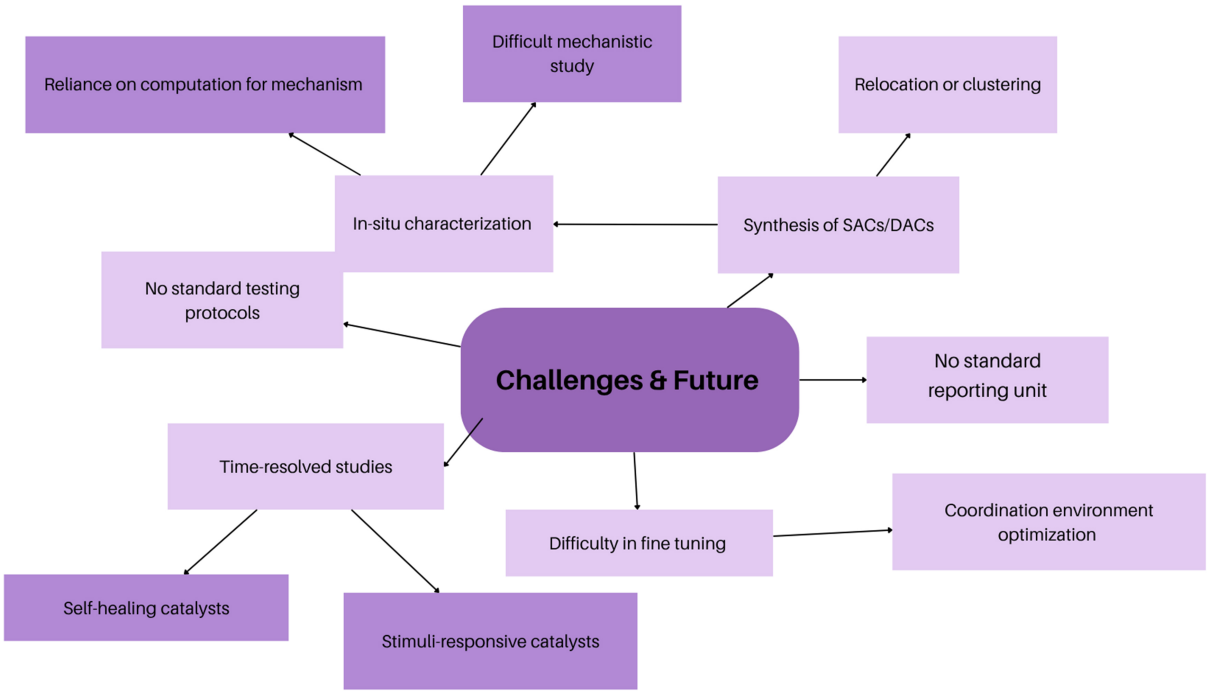

Figure 7. Mind-map of challenges and outlook of SACs and DACs for NRA. SACs: Single-atom catalysts; DACs: dual-atom catalysts; NRA: nitrate reduction to ammonia.

measurements using a suitable interface, all structural changes can be tracked during catalysis[120]. Material scientists, analytical chemists, and engineers need to work together in this direction.

The future lies in responsive materials. Instead of static structures, scientists should aim to design SACs/DACs that are responsive to pH, the concentration of specific species, applied potentials and temperature. Thus, variations in these factors can change the coordination environment of metal atoms, allowing them to adsorb intermediates accordingly at low energies[76]. Furthermore, catalyst activity is often diffusion limited. To overcome this, autonomous self-propelled micro- and nanorobots are gaining popularity. SACs/DACs can be converted into nanorobots to self-propel in areas of high nitrate concentration and carry out NRA effectively[121].

A further outlook includes the practical implementation of SACs/DACs for NRA on an industrial and commercial scale, through integration with membrane electrode assemblies (MEAs). Shen *et al.* designed an NRA continuous flow electrolysis cell integrated with a membrane separator[71]. This achieved an ammonia production rate of 325.9 $mg_N \cdot h^{-1} \cdot g_{Cu}^{-1}$ with 98.3% collection efficiency at an energy consumption of 17.11 $kWh \cdot g_N^{-1}$. This work highlights that coupling SACs/DACs with MEA is highly feasible and demonstrates potential for scalability.

During catalysis, structure reconstruction takes place, which decreases the activity of SACs/DACs. There is a need for in-operando regeneration methods to reverse these reconstructions. For instance, oxidative pulses can regenerate vacancies, and a reducing environment can relocate dopants. Such maintenance could sustain SACs/DACs over longer time periods. For example, Cu and Ti oxide-based nanofibers were designed to undergo *in-situ* electrochemical reduction to stabilize Cu^+ active sites. This increased catalyst stability over 50 cycles with nitrate removal efficiency exceeding 90%[122]. Such self-healing materials need to be explored for SACs/DACs as they can undergo reversible structural changes, thereby enabling *in-situ* modulation of intermediate adsorption and nitrate reduction kinetics under variable operating conditions. A mind-map of current challenges and future goals have been elaborated in Figure 7.

CONCLUSION

This review summarizes and critically discusses recent research on SACs and DACs for NRA, offering a parallel comparison of these catalysts. It focuses on the choice of metals and the coordination environment variables, and on how these factors tune the electronic structure, reaction mechanism, intermediate stabilization, and selectivity, activity, and stability of catalyst. This review also elaborates on how metal-metal synergistic effects in DACs, along with the complicated interplay of coordination asymmetry, unsaturation, heteroatom dopants, and experimental operators like potential and pH, control catalytic performance. The computational studies, software packages, and simulations used, as well as the future directions of DFT and machine learning in SACs/DACs, are also discussed. Furthermore, challenges in the field are highlighted, and viable solutions along with a clear roadmap for future research are critically suggested to advance work in this field.

DECLARATIONS

Authors' contributions

Wrote the original draft, conceptualized the study, and performed methodology, investigation, and formal analysis: Tahir, N.

Performed visualization, validation, software, methodology, investigation, and acquired funding: Guo, P.

Performed visualization, validation, and software: Fatima, T.

Performed visualization, validation, software, methodology, investigation, formal analysis, and contributed to conceptualization: Nazir, M. A.

Performed visualization, validation, investigation, formal analysis, and contributed to conceptualization: Pervaiz, K.

Performed visualization, validation, software, methodology, investigation, and formal analysis: Shaheen, S.

Curated data, contributed to conceptualization, and performed visualization, validation, software, investigation, and formal analysis: Murtaza, G.

Curated data, reviewed and edited the manuscript, contributed to conceptualization, and performed visualization, validation, software, methodology, investigation, and formal analysis: Najam, T.; Cai, X.

Supervised the whole project, provided resources, reviewed and edited the manuscript, and performed visualization, validation, software, methodology, investigation, and conceptualization: Shah, S. S. A.

Availability of data and materials

Not applicable.

AI and AI-assisted tools statement

Not applicable.

Financial support and sponsorship

This work was supported by the NUST-Flagship Project (FSP-23-08), Pakistan Science Foundation (PSF-NSFC-V/ENG/C-NUST/36), Science and Technology Innovation Commission of Shenzhen (No. JCYJ20240813142620027), Natural Science Foundation of China (No. 52373266), and Guangdong Basic and Applied Basic Research Foundation (No. 2024A1515012334).

Conflicts of interest

All authors declared that there are no conflicts of interest.

Ethical approval and consent to participate

Not applicable.

Consent for publication

Not applicable.

REFERENCES

1. Wang, J.; Chen, J.; Jin, Z.; et al. Simultaneous removal of phosphate and ammonium nitrogen from agricultural runoff by amending soil in lakeside zone of Karst area, Southern China. *Agric. Ecosyst. Environ.* **2020**, *289*, 106745. DOI
2. Herbinet, O.; Bartocci, P.; Grinberg Dana, A. On the use of ammonia as a fuel - a perspective. *Fuel. Commun.* **2022**, *11*, 100064. DOI
3. Sun, S.; Jiang, Q.; Zhao, D.; et al. Ammonia as hydrogen carrier: advances in ammonia decomposition catalysts for promising hydrogen production. *Renew. Sustain. Energy. Rev.* **2022**, *169*, 112918. DOI
4. Shen, H.; Choi, C.; Masa, J.; et al. Electrochemical ammonia synthesis: mechanistic understanding and catalyst design. *Chem* **2021**, *7*, 1708-54. DOI
5. Bijay-Singh; Craswell, E. Fertilizers and nitrate pollution of surface and ground water: an increasingly pervasive global problem. *SN. Appl. Sci.* **2021**, *3*, 518. DOI
6. Yao, Y.; Wei, K.; Zhao, S.; et al. Highly efficient bifunctional NiFe-MOF array electrode for nitrate reduction to ammonia and oxygen evolution reactions. *ACS. Sustain. Chem. Eng.* **2025**, *13*, 1245-52. DOI
7. Zou, Y.; Yan, Y.; Xue, Q.; et al. MOF-on-MOF heterostructured electrocatalysts for efficient nitrate reduction to ammonia. *Angew. Chem. Int. Ed. Engl.* **2024**, *63*, e202409799. DOI PubMed
8. Meng, X.; Tan, X.; Ma, Y.; et al. Recent progress in cobalt-based electrocatalysts for efficient electrochemical nitrate reduction reaction. *Adv. Funct. Mater.* **2025**, *35*, 2418492. DOI
9. Zhou, J.; Gao, S.; Hu, G. Recent progress and perspectives on transition metal-based electrocatalysts for efficient nitrate reduction. *Energy. Fuels.* **2024**, *38*, 6701-22. DOI
10. Wei, X.; Chen, C.; Fu, X.; Wang, S. Oxygen vacancies-rich metal oxide for electrocatalytic nitrogen cycle. *Adv. Energy. Mater.* **2024**, *14*, 2303027. DOI
11. Wu, Q.; Zhu, W.; Ma, D.; Liang, C.; Wang, Z.; Liang, H. Screening of transition metal oxides for electrocatalytic nitrate reduction to ammonia at large currents. *Nano. Res.* **2024**, *17*, 3902-10. DOI
12. Fan, Y.; Wang, X.; Butler, C.; et al. Highly efficient metal-free nitrate reduction enabled by electrified membrane filtration. *Nat. Water.* **2024**, *2*, 684-96. DOI
13. Ahmad, M. S.; Rasheed, T. Water-stable MOFs and composites: a greener and sustainable approach for enhanced reactivity towards the electrochemical nitrate reduction reaction. *J. Mater. Chem. A.* **2025**, *13*, 16309-29. DOI
14. Liu, L.; Zheng, S. Advancements in single atom catalysts for electrocatalytic nitrate reduction reaction. *ChemCatChem* **2024**, *16*, e202301641. DOI
15. Lv, L.; Shen, Y.; Zhou, M.; et al. High-throughput screening for efficient dual-atom catalysts in electrocatalytic nitrate reduction to ammonia *via* dissociation–association mechanism. *J. Mater. Chem. A.* **2024**, *12*, 6733-46. DOI
16. Shan, J.; Ye, C.; Jiang, Y.; Jaroniec, M.; Zheng, Y.; Qiao, S. Z. Metal-metal interactions in correlated single-atom catalysts. *Sci. Adv.* **2022**, *8*, eabo0762. DOI PubMed PMC
17. Zhang, Z.; Li, H.; Wu, D.; et al. Coordination structure at work: atomically dispersed heterogeneous catalysts. *Coord. Chem. Rev.* **2022**, *460*, 214469. DOI
18. Liang, X.; Yao, S.; Li, Z.; Li, Y. Challenge and chance of single atom catalysis: the development and application of the single atom site catalysts toolbox. *Acc. Chem. Res.* **2025**, *58*, 1607-19. DOI
19. Najam, T.; Shah, S. S. A.; Yin, H.; et al. Second-shell modulation on porphyrin-like Pt single atom catalysts for boosting oxygen reduction reaction. *Chem. Sci.* **2024**, *15*, 18513-23. DOI PubMed PMC
20. Yuan, Z.; Cheng, M.; Tong, J.; et al. Explosive advances of metal-organic frameworks-derived single atom catalysts modified by metal species in diverse sizes for electrocatalysis: synthesis, collaboration, and mechanism. *Coord. Chem. Rev.* **2026**, *548*, 217167. DOI
21. Shah, S. S. A.; Kazmi, J.; Nazir, M. A.; et al. Synergistic Ni single-atom–nanoparticle interfaces for poison-resistant CO_2 electroreduction. *Chem. Eng. J.* **2026**, *527*, 172062. DOI
22. Roy, S.; Singh, J. K. Heptazine-based g-C_3N_4-supported efficient single atom electrocatalysts for HER/OER/ORR: a first-principles study. *Int. J. Hydrogen. Energy.* **2026**, *198*, 152680. DOI
23. Yan, C.; Zhang, W.; Ye, J.; Li, X.; Deng, Q. Metal-free bifunctional catalysis on carbon-doped o-B_2N_2: site-dependent activity for ORR and OER. *Int. J. Hydrogen. Energy.* **2026**, *198*, 152601. DOI
24. Li, X.; Ding, Q.; He, J.; et al. Asymmetric Fe single atom on BN for boosted nitrate electroreduction to ammonia. *J. Mater. Chem. A.* **2026**, *14*, 2825-34. DOI
25. Wu, X.; Chen, Y.; Tang, B.; et al. CeO_x-integrated dual site enhanced urea electrosynthesis from nitrate and carbon dioxide. *Nat. Commun.* **2025**, *16*, 8785. DOI PubMed PMC
26. Zhou, P.; Ruan, W.; Zhou, T.; Guan, J. Advancements in dual-atom-site catalysts for electrocatalysis. *Nano. Res.* **2026**, *19*, 94907996. DOI

27. Lin, B.; Lo, T. W. B. Engineering isolated and paired active metal sites on MOFs for photocatalytic CO_2 reduction. *Coord. Chem. Rev.* **2026**, *549*, 217329. DOI
28. Li, Q.; Wang, L.; Wu, J. Recent advances in dual-atom catalysts for energy catalysis. *Rare. Met.* **2025**, *44*, 841-67. DOI
29. Zhang, M.; Cao, X.; Dong, J.; Zhu, X.; Zhu, Y.; Wang, L. Unveiling the mystery of precision catalysis: dual-atom catalysts stealing the spotlight. *Small* **2025**, *21*, e2409560. DOI PubMed
30. Sun, J.; Tang, T.; Zhang, S.; et al. A dual-atom La_2 catalyst for the oxygen reduction reaction. *Angew. Chem. Int. Ed. Engl.* **2025**, *64*, e202509063. DOI PubMed
31. Yan, L.; Mao, Y.; Li, Y.; et al. Sublimation transformation synthesis of dual-atom Fe catalysts for efficient oxygen reduction reaction. *Angew. Chem. Int. Ed. Engl.* **2025**, *64*, e202413179. DOI PubMed
32. Subhadarshini, S.; Pumera, M. Single atom catalyst for nitrate-to-ammonia electrochemistry. *Small* **2025**, *21*, e2403515. DOI PubMed PMC
33. Yin, S.; Wang, Y. Single-atom catalysts for electrochemical nitrate reduction to ammonia: rational design, mechanistic insights, and system perspectives. *Catalysts* **2025**, *15*, 1084. DOI
34. Zhao, D.; Jia, Y.; Wang, H.; Liu, S.; Zhang, W.; Fan, J. Electrocatalytic nitrate reduction to ammonia over single-atom catalysts: focus on support materials. *Sep. Purif. Technol.* **2025**, *377*, 134420. DOI
35. Yang, Y.; Zhu, J.; Li, W.; et al. Recent advances in single-atom catalysts for electrochemical nitrate reduction to ammonia. *J. Environ. Chem. Eng.* **2025**, *13*, 115144. DOI
36. Cao, Y.; Yuan, S.; Meng, L.; et al. Recent advances in electrocatalytic nitrate reduction to ammonia: mechanism insight and catalyst design. *ACS. Sustain. Chem. Eng.* **2023**, *11*, 7965-85. DOI
37. Xiang, T.; Liang, Y.; Zeng, Y.; et al. Transition metal single-atom catalysts for the electrocatalytic nitrate reduction: mechanism, synthesis, characterization, application, and prospects. *Small* **2023**, *19*, e2303732. DOI PubMed
38. Niu, H.; Zhang, Z.; Wang, X.; Wan, X.; Shao, C.; Guo, Y. Theoretical insights into the mechanism of selective nitrate-to-ammonia electroreduction on single-atom catalysts. *Adv. Funct. Mater.* **2021**, *31*, 2008533. DOI
39. Cheng, X.; Shang, W.; Li, Y.; et al. Unveiling structural evolution of Fe single atom catalyst in nitrate reduction for enhanced electrocatalytic ammonia synthesis. *Nano. Res.* **2024**, *17*, 6826-32. DOI
40. Wu, Z. Y.; Karamad, M.; Yong, X.; et al. Electrochemical ammonia synthesis via nitrate reduction on Fe single atom catalyst. *Nat. Commun.* **2021**, *12*, 2870. DOI PubMed PMC
41. Zhang, X.; Liu, X.; Huang, Z. F.; et al. Regulating intermediate adsorption and H_2O dissociation on a diatomic catalyst to promote electrocatalytic nitrate reduction to ammonia. *Energy. Environ. Sci.* **2024**, *17*, 6717-27. DOI
42. Yin, S.; Wang, Y. Progress and challenges in the electrocatalytic reduction of nitrate to ammonia. *Molecules* **2025**, *30*, 3910. DOI PubMed PMC
43. Zhong, W.; Chen, Y.; Chen, P.; et al. Balancing hydrogen evolution and hydrogenation reaction via facet engineering for efficient conversion of nitrate to ammonia in actual wastewater. *Angew. Chem. Int. Ed. Engl.* **2025**, *64*, e202503117. DOI PubMed
44. Qiu, L.; Liu, F.; Liu, S.; et al. Subnanometric Pt cluster induced hydrogenation of nitrogen-intermediate species for ammonia electrosynthesis on bimetallic Pt/Cu catalyst. *Appl. Catal. B. Environ. Energy.* **2026**, *384*, 126151. DOI
45. Zhao, T.; Yang, M.; Sun, Y.; Wang, Z.; Cai, Q.; Zhao, J. High-throughput screening of highly efficient Cu-based dual-atom catalysts to promote nitrate electroreduction for ammonia synthesis: a computational study. *Mol. Catal.* **2023**, *541*, 113095. DOI
46. Wang, Y.; Tang, C.; Li, Q.; Xiao, T.; Xiong, F. Theoretical prediction of efficient Cu-based dual-atom alloy catalysts for electrocatalytic nitrate reduction to ammonia via high-throughput first-principles calculations. *J. Mater. Chem. A.* **2025**, *13*, 3765-76. DOI
47. Chen, H.; Li, J.; Shi, R.; et al. Coupled $Pd^{\delta-}$-$Cu^{\delta+}$ dipole for enhanced aqueous nitrate valorization at ultralow potentials. *ACS. Nano.* **2025**, *19*, 31677-89. DOI PubMed
48. Wan, J.; Zhang, H.; Yang, J.; et al. Synergy between Fe and Mo single atom catalysts for ammonia electrosynthesis. *Appl. Catal. B. Environ. Energy.* **2024**, *347*, 123816. DOI
49. Xiao, H.; Lv, Y.; Hua, W.; et al. Atomically dispersed dual frustrated Lewis pairs for efficient relay conversion of nitrate into ammonia. *Appl. Catal. B. Environ. Energy.* **2025**, *377*, 125501. DOI
50. Xu, H.; Peng, J.; Li, P.; et al. Gradient adsorption energy strategy unlocks ultra-long stability and efficient electrocatalytic ammonia synthesis from nitrate over CoP/Cu_3P. *Angew. Chem. Int. Ed. Engl.* **2026**, *65*, e22410. DOI PubMed
51. Zhang, S.; Wu, J.; Zheng, M.; et al. Fe/Cu diatomic catalysts for electrochemical nitrate reduction to ammonia. *Nat. Commun.* **2023**, *14*, 3634. DOI PubMed PMC
52. Liu, K.; Sun, Z.; Peng, X.; et al. Tailoring asymmetric RuCu dual-atom electrocatalyst toward ammonia synthesis from nitrate. *Nat. Commun.* **2025**, *16*, 2167. DOI PubMed PMC

53. Song, J.; Qian, S.; Yang, W.; et al. Nano-single-atom heterointerface engineering for pH-universal electrochemical nitrate reduction to ammonia. *Adv. Funct. Mater.* **2024**, *34*, 2409089. DOI
54. Sun, Y.; Feng, G.; Wang, Z.; et al. Atomic-level tailoring of single-atom tungsten catalysts for optimized electrochemical nitrate-to-ammonia conversion. *J. Colloid. Interface. Sci.* **2024**, *676*, 1023-31. DOI PubMed
55. Yang, X.; Yang, J.; Zheng, X.; et al. Enzyme-mimetic single-atom catalyst design for green ammonia synthesis. *Adv. Energy. Mater.* **2025**, *15*, 2501867. DOI
56. Ni, J.; Yan, J.; Li, F.; et al. Atomic Co–P catalytic pair drives efficient electrochemical nitrate reduction to ammonia. *Adv. Energy. Mater.* **2024**, *14*, 2400065. DOI
57. Chang, G.; Chen, X.; Lv, J. J.; Kong, Z.; Wang, Z. J. Cobalt-based electrocatalysts for sustainable nitrate conversion: structural design and mechanistic advancements. *Nanomicro. Lett.* **2025**, *18*, 73. DOI PubMed PMC
58. Wang, S.; Gao, H.; Li, L.; et al. High-throughput identification of highly active and selective single-atom catalysts for electrochemical ammonia synthesis through nitrate reduction. *Nano. Energy.* **2022**, *100*, 107517. DOI
59. Shang, S.; Wang, F.; Sun, Z.; Qiang, C.; Chu, K. Electrocatalytic nitrite reduction to ammonia on isolated bismuth alloyed ruthenium. *J. Energy. Chem.* **2025**, *100*, 369-76. DOI
60. Zhao, T.; Chen, K.; Xu, X.; et al. Homonuclear dual-atom catalysts embedded on N-doped graphene for highly efficient nitrate reduction to ammonia: from theoretical prediction to experimental validation. *Appl. Catal. B. Environ.* **2023**, *339*, 123156. DOI
61. Sathishkumar, N.; Chen, H. Mechanistic understanding of the electrocatalytic nitrate reduction activity of double-atom catalysts. *J. Phys. Chem. C.* **2023**, *127*, 994-1005. DOI
62. Li, Y.; Feng, Q.; László, K.; Wang, Y. High-throughput screening of high C/N-ratio homonuclear dual-atom catalysts for electrochemical reduction of nitrate to ammonia. *Chin. Chem. Lett.* **2026**, *37*, 111536. DOI
63. Pandiyan, K.; Chen, H. Design principles of biphenylene-supported dual-atom catalysts for efficient and selective nitrate reduction to ammonia. *J. Mater. Chem. A.* **2026**, *14*, 1245-59. DOI
64. Wang, Y.; Tang, C.; Xiao, T.; et al. High-throughput screening of trimetallic dual-atom alloy catalysts for electrocatalytic nitrate reduction to ammonia. *J. Energy. Chem.* **2025**, *110*, 728-39. DOI
65. Zhang, J.; Xia, H.; Jiang, K.; et al. High-efficiency nitrate reduction to nitrogen using PdCu dual-atom electrocatalysts anchored on nitrogen-doped carbon. *Chem. Eng. J.* **2025**, *519*, 165362. DOI
66. Meng, X.; Wang, K.; Zhao, Z.; Li, K.; Sun, W.; Lin, Y. Preventing nitrite desorption via switching hydrogenation position: a dual-site approach for selective nitrate reduction to ammonia. *Small* **2025**, *21*, e2407216. DOI PubMed
67. Zhao, G.; Yu, M.; He, C. Theoretical study of nitrate reduction to ammonia on dual-atom doped CoP(101) catalysts. *Surfaces. Interfaces.* **2025**, *75*, 107859. DOI
68. Wei, J.; Li, C.; Sun, Z.; et al. Nitrogen-rich MOF-material-derived metal dual-atom platforms for efficient electrochemical nitrate reduction. *Angew. Chem. Int. Ed. Engl.* **2025**, *137*, e202517259. DOI PubMed
69. Park, J.; Theerthagiri, J.; Yodsin, N.; Limphirat, W.; Junmon, P.; Choi, M. Y. CO_2 laser-stabilized Ni-Co dual single-atomic sites for energy generation and ammonia harvesting. *Adv. Mater.* **2025**, *37*, e2506137. DOI PubMed
70. Feng, C.; Bo, K.; Wan, J.; Zhang, H.; Wang, Y. Triple synergy engineering via metal-free dual-atom incorporation for self-sustaining acidic ammonia electrosynthesis. *Angew. Chem. Int. Ed. Engl.* **2025**, *64*, e202505211. DOI PubMed
71. Shen, F.; He, S.; Tang, X.; et al. Breaking linear scaling relation limitations on a dual-driven single-atom copper-tungsten oxide catalyst for ammonia synthesis. *Angew. Chem. Int. Ed. Engl.* **2025**, *64*, e202423154. DOI PubMed
72. Ren, Y.; Wang, J.; Yang, L.; et al. Single-atom Cu and Zn vacancy synergy in NiFe-LDH boosts metal-support interaction for high-efficiency nitrate-to-ammonia electroreduction. *Environ. Sci. Technol.* **2025**, *59*, 11414-25. DOI PubMed
73. Zhang, Y.; Yang, J.; Ge, R.; et al. The effect of coordination environment on the activity and selectivity of single-atom catalysts. *Coord. Chem. Rev.* **2022**, *461*, 214493. DOI
74. Murphy, E.; Liu, Y.; Matanovic, I.; et al. Elucidating electrochemical nitrate and nitrite reduction over atomically-dispersed transition metal sites. *Nat. Commun.* **2023**, *14*, 4554. DOI PubMed PMC
75. Huang, J.; Hu, S.; Liu, M.; et al. Single-, double-, and triple-atom catalysts on PC_6 for nitrate reduction to ammonia: a computational screening. *Electrochim. Acta.* **2024**, *504*, 144915. DOI
76. Zhang, S.; Zhang, R.; Guo, Y.; Zhi, C. Ammonia synthesis from nitrate reduction by the modulation of a built-in electric field and external stimuli. *EES. Catal.* **2025**, *3*, 235-53. DOI
77. Mo, Z.; Mu, J.; Liu, B. Transition metal single-atom electrocatalytic reduction catalyst for nitrate to ammonia. *J. Electroanal. Chem.* **2024**, *969*, 118533. DOI
78. Sathishkumar, N.; Wu, S.; Chen, H. Mechanistic exploring the catalytic activity of single-atom catalysts anchored in graphitic carbon nitride toward electroreduction of nitrate-to-ammonia. *Appl. Surf. Sci.* **2022**, *598*, 153829. DOI

79. Xu, L.; Ding, T.; Sun, Y.; et al. Reversed intermediate conformation on heteronuclear atomic sites for promoted electrocatalytic nitrate reduction to ammonia. *Appl. Catal. B. Environ. Energy.* **2025**, *379*, 125680. DOI
80. Zhao, X.; Geng, Q.; Dong, F.; et al. Boosting the selectivity and efficiency of nitrate reduction to ammonia with a single-atom Cu electrocatalyst. *Chem. Eng. J.* **2023**, *466*, 143314. DOI
81. Chen, X.; Ji, X.; Kou, J. Rational design of iron single-atom catalysts for electrochemical nitrate reduction to produce ammonia. *Discov. Chem. Eng.* **2023**, *3*, 38. DOI
82. Li, Q.; Li, Y.; Xu, B.; Yang, J.; Wang, Y. Gram-scale ammonia synthesis via electrochemical nitrate reduction using enzyme-inspired dual-atomic Cu catalyst. *Angew. Chem. Int. Ed. Engl.* **2025**, *64*, e202510139. DOI PubMed
83. Wan, J.; Yang, J.; Yang, N.; et al. Axial chlorine-induced symmetry-breaking iron single-atom catalyst for electrochemical ammonia synthesis. *ACS. Catal.* **2025**, *15*, 4507-18. DOI
84. Xue, Y.; Yu, Q.; Ma, Q.; et al. Electrocatalytic hydrogenation boosts reduction of nitrate to ammonia over single-atom Cu with Cu(I)-N_3C_1 sites. *Environ. Sci. Technol.* **2022**, *56*, 14797-807. DOI PubMed
85. Liu, X.; Xiang, T.; Liang, Y.; et al. When electrocatalytic nitrate reduction meets copper-based atomic site catalysts. *J. Mater. Chem. A.* **2024**, *12*, 26367-89. DOI
86. Lian, Z.; Luo, D.; Yang, J.; et al. Spatial decoupling of adsorption and transformation sites on Ag-Cu dual-single-atom catalysts for highly selective photocatalytic nitrate-to-ammonia reduction. *Angew. Chem. Int. Ed. Engl.* **2026**, *65*, e202516964. DOI PubMed
87. Yin, Y.; Wang, L.; Shang, H.; Zhang, X.; Chen, W.; Zou, X. Lateral coordination sulfur-modified charge asymmetry Cu-Ru diatomic catalyst for efficient and stable electrochemical nitrate reduction to ammonia. *ACS. Nano.* **2025**, *19*, 30338-48. DOI PubMed
88. Qi, Y.; Hou, X.; He, Z.; et al. Phosphorus-doped $Ti_3C_2T_x$ MXene nanosheets enabling ambient NH_3 synthesis with high current densities. *Chem. Commun.* **2024**, *60*, 8728-31. DOI
89. Cui, Z.; Wang, H.; Li, C.; Peng, W.; Liu, J. Iodine dopants facilitate tandem catalysis via transformation adsorption behavior for efficient electrochemical nitrate reduction reaction. *ACS. Nano.* **2025**, *19*, 31050-64. DOI PubMed
90. Cai, J.; Wei, Y.; Cao, A.; et al. Electrocatalytic nitrate-to-ammonia conversion with ~100% Faradaic efficiency via single-atom alloying. *Appl. Catal. B. Environ.* **2022**, *316*, 121683. DOI
91. Zhang, M.; Cheng, X.; Duan, Y.; Chen, J.; Wang, Y. Q. Boron doping induced strong anchor effect between bimetal NiCo alloy and carbon support for efficient electrocatalytic nitrate reduction to ammonia. *ChemSusChem* **2025**, *18*, e202401979. DOI
92. Zhang, Y.; Su, K.; Huang, B. Heteroatom-doping-engineered spin state of single-atom Fe on MXene for electrocatalytic NO-to-NH_3 conversion. *Appl. Surf. Sci.* **2026**, *720*, 165264. DOI
93. Xiong, Y.; Wang, Y.; Zhou, J.; Liu, F.; Hao, F.; Fan, Z. Electrochemical nitrate reduction: ammonia synthesis and the beyond. *Adv. Mater.* **2024**, *36*, e2304021. DOI PubMed
94. Chao, G.; Wang, J.; Zong, W.; et al. Single-atom catalysts for electrocatalytic nitrate reduction into ammonia. *Nanotechnology* **2024**, *35*, 432001. DOI PubMed
95. Xu, X.; Guan, J. Metal-organic-framework-derived dual-atom catalysts: from synthesis to electrocatalytic applications. *Mater. Sci. Eng. R. Rep.* **2025**, *162*, 100886. DOI
96. Zhu, T.; Chen, Q.; Liao, P.; et al. Single-atom Cu catalysts for enhanced electrocatalytic nitrate reduction with significant alleviation of nitrite production. *Small* **2020**, *16*, e2004526. DOI PubMed
97. Zhang, S.; Jiang, Q.; Shi, T.; et al. Laser irradiation in liquid to release cobalt single-atom sites for efficient electrocatalytic N_2 reduction. *ACS. Appl. Energy. Mater.* **2020**, *3*, 6079-86. DOI
98. Sha, Y.; Moissinac, F.; Zhu, M.; et al. Laser synthesis of nonprecious metal-based single-atom catalysts for oxygen reduction reaction. *ACS. Appl. Mater. Interfaces.* **2023**, *15*, 51004-12. DOI PubMed
99. Goyal, N.; Li, F.; Hu, Y. Tailoring single-metal atom catalysts: a strategic defect engineering approach for electrochemical reduction reactions. *J. Mater. Chem. A.* **2024**, *12*, 19685-719. DOI
100. Xue, Z.; Tan, R.; Tian, J.; Hou, H.; Zhang, X.; Zhao, Y. Ab initio study of a tandem PdCu catalyst supported on carbon nitride nanosheets for nitrate-to-ammonia electrochemical reduction. *ACS. Appl. Nano. Mater.* **2025**, *8*, 1709-17. DOI
101. Wang, J.; Liao, K.; Wei, Y.; et al. Ru–B modulated electronic structure promotes electrocatalytic nitrate reduction to ammonia and zinc-nitrate battery. *Adv. Funct. Mater.* **2026**, *36*, e16068. DOI
102. Braga, D. S.; Pedersen, A.; Riyaz, M.; et al. In situ structural evolution and activity descriptor of atomically dispersed catalysts during nitrate electroreduction. *Adv. Sci.* **2025**, *12*, e10282. DOI PubMed PMC
103. Maeng, J.; Heo, J.; Kwak, M.; et al. Dual atom Cu–Fe ensemble sites for enhanced efficiency of green ammonia production from the tandem electrochemical nitrate reduction process. *J. Mater. Chem. A.* **2026**, *14*, 7608-18. DOI
104. Zhang, W.; Dong, H.; Zhou, L.; et al. Fe single-atom catalysts with pre-organized coordination structure for efficient electrochemical nitrate reduction to ammonia. *Appl. Catal. B. Environ.* **2022**, *317*, 121750. DOI

105. Liu, D.; Qiao, L.; Peng, S.; et al. Recent advances in electrocatalysts for efficient nitrate reduction to ammonia. *Adv. Funct. Mater.* **2023**, *33*, 2303480. DOI

106. Xu, L.; Liu, W.; Liu, K. Single atom environmental catalysis: influence of supports and coordination environments. *Adv. Funct. Mater.* **2023**, *33*, 2304468. DOI

107. Li, Z.; Yang, C.; Xu, B.; Yao, L.; Zhu, W.; Cui, Y. Electrochemically nitrate remediation by single-atom catalysts: advances, mechanisms, and prospects. *Energy. Mater.* **2024**, *4*, 400046. DOI

108. Qian, S. J.; Cao, H.; Wang, Y. G.; Li, J. Controlling the selectivity of electrocatalytic NO reduction through pH and potential regulation on single-atom catalysts. *J. Am. Chem. Soc.* **2024**, *146*, 12530-7. DOI PubMed

109. Nittoor-Veedu, R.; Ju, X.; Langer, M.; Gao, W.; Otyepka, M.; Pumera, M. Periodic table exploration of MXenes for efficient electrochemical nitrate reduction to ammonia. *Small* **2025**, *21*, e2410105. DOI PubMed PMC

110. Dong, K.; Han, S.; Li, Y.; et al. Testing, quantification, in situ characterization and calculation simulation for electrocatalytic nitrate reduction. *Nat. Protoc.* **2026**, *21*, 2707-62. DOI PubMed

111. Liu, J.; Xu, Y.; Duan, R.; et al. Reaction-driven formation of anisotropic strains in FeTeSe nanosheets boosts low-concentration nitrate reduction to ammonia. *Nat. Commun.* **2025**, *16*, 3595. DOI PubMed PMC

112. Moore, J. M.; Miller, T. J.; Mu, M.; et al. Selective stepwise reduction of nitrate and nitrite to dinitrogen or ammonia. *J. Am. Chem. Soc.* **2025**, *147*, 8444-54. DOI PubMed PMC

113. Chen, L. L.; Yu, W.; Wang, Y.; et al. High-yield ammonia production from Al-nitrate battery via anodic Al&NO_3^- spontaneous reaction driven cathodic nitrate reduction reaction. *Adv. Mater.* **2026**, *38*, e16520. DOI PubMed

114. Zhong, D. C.; Wang, Y. C.; Wang, M.; Lu, T. B. Precise synthesis of dual-atom catalysts for better understanding the enhanced catalytic performance and synergistic mechanism. *Acc. Chem. Res.* **2025**, *58*, 1379-91. DOI

115. Qiao, M.; Zhu, D.; Guo, C. Advances in designing efficient electrocatalysts for nitrate reduction from a theoretical perspective. *Chem. Commun.* **2024**, *60*, 11642-54. DOI

116. Hu, Y.; Lan, H.; He, J.; et al. Entropy-engineered middle-in synthesis of dual single-atom compounds for nitrate reduction reaction. *ACS. Nano.* **2024**, *18*, 23168-80. DOI PubMed

117. Liang, H.; Wang, J.; Qiao, Z.; Li, Y.; Wang, C. Machine-learning-assisted design of novel metallic 2D C_3N_3 supported single/double atom catalysts for nitrogen reduction reaction. *Appl. Surf. Sci.* **2025**, *689*, 162451. DOI

118. Chen, X.; Cheng, H.; Shi, R.; Zhou, T.; He, T.; Liu, Q. Recent advances in data-driven design of dual-atom catalysts. *Adv. Funct. Mater.* **2026**, *36*, e10647. DOI

119. Zhou, X.; Tamtaji, M.; Zhou, W.; Goddard, W. A. 3rd.; Chen, G. Nonprecious triple-atom catalysts with ultrahigh activity for electrochemical reduction of nitrate to ammonia: a DFT screening. *ACS. Appl. Mater. Interfaces.* **2025**, *17*, 4854-64. DOI PubMed PMC

120. Liu, Y.; Su, X.; Ding, J.; et al. Progress and challenges in structural, *in situ* and *operando* characterization of single-atom catalysts by X-ray based synchrotron radiation techniques. *Chem. Soc. Rev.* **2024**, *53*, 11850-87. DOI

121. Tahir, N.; Najam, T.; Nazir, M. A.; et al. Metal-organic frameworks: nanomachines for efficient water purification. *Chin. Chem. Lett.* **2026**, *37*, 112326. DOI

122. Cong, Y.; Kang, X.; Wu, Z.; et al. Self-reconstruction induced electronic metal-support interaction for modulated Cu^+ sites on TiO_2 nanofibers in electrocatalytic nitrate conversion. *Small* **2024**, *20*, e2407554. DOI PubMed